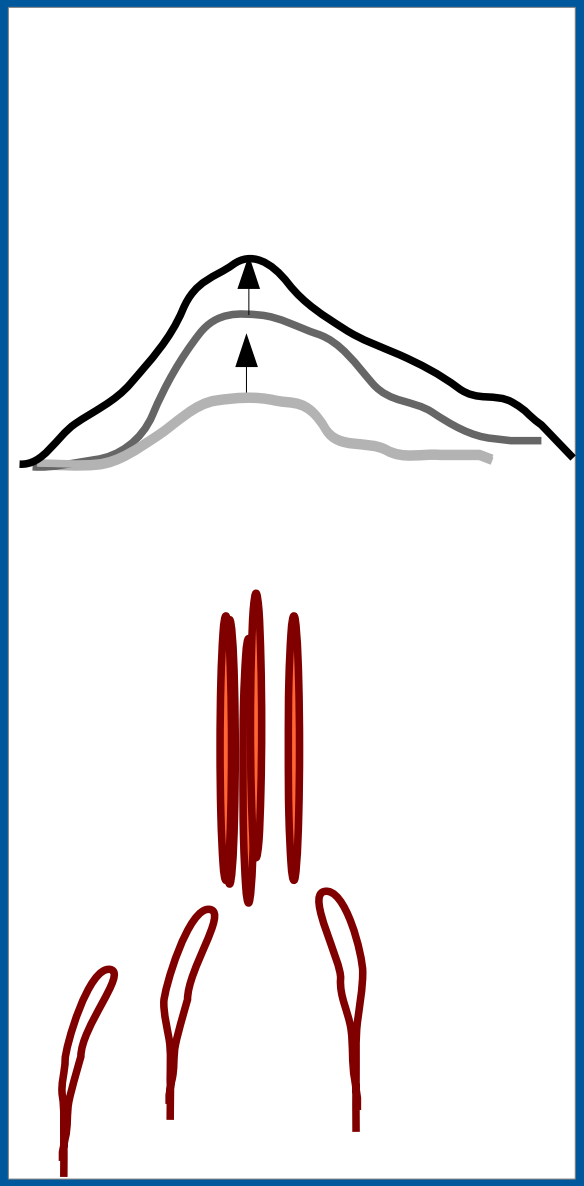

Magma storage depth and shape and eruption size controlled top-down by surface loads

Eleonora Rivalta

Conceptual models of reservoir formation

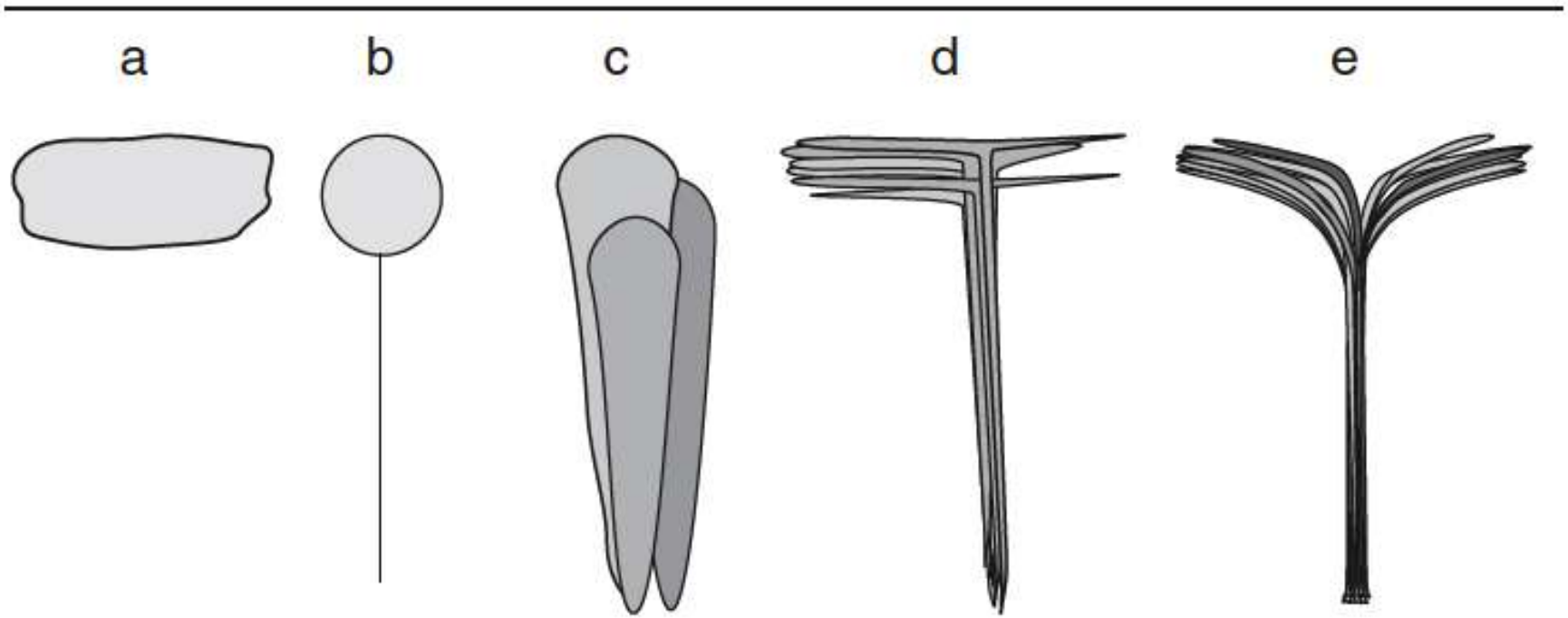

a) Large crystalline mushes b) Geodesy view of a magma chamber as a pressurized sphere or ellipsoid;

c) Formation through accumulation of plutons;
d) Formation through accumulation of sills;
e) Funnel-shaped intrusions resulting from a change of stress close to the surface (from Annen et al., 2015).

Stress due to volcano edifice loading

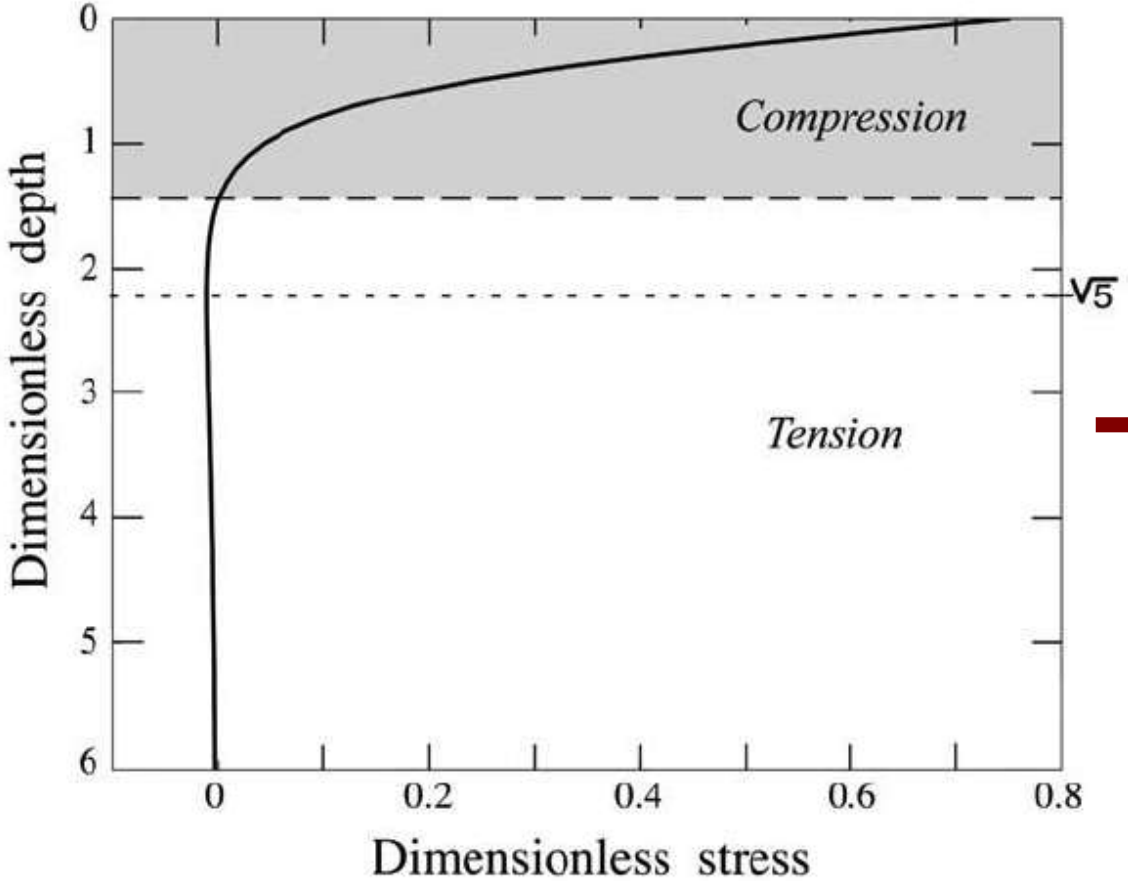

Magma storage depth and composition change following edifice construction and destruction events

Normal stress at the axis due to a flat edifice as a function of depth. With increasing depth, the edifice induces compression and then tension. Tensile stresses are largest at dimensionless depth z=sqrt(5)

From Pinel and Jaupart, 2004

Outline

Edifice history (construction, flank collapse, deglaciation, drainage of summit lake, caldera formation...)

Surface load changes

Tectonics (crustal thinning, orogenesis, fault scarp development...)

Magma storage depth & shape
Typical eruption size

Loading due to a volcanic edifice

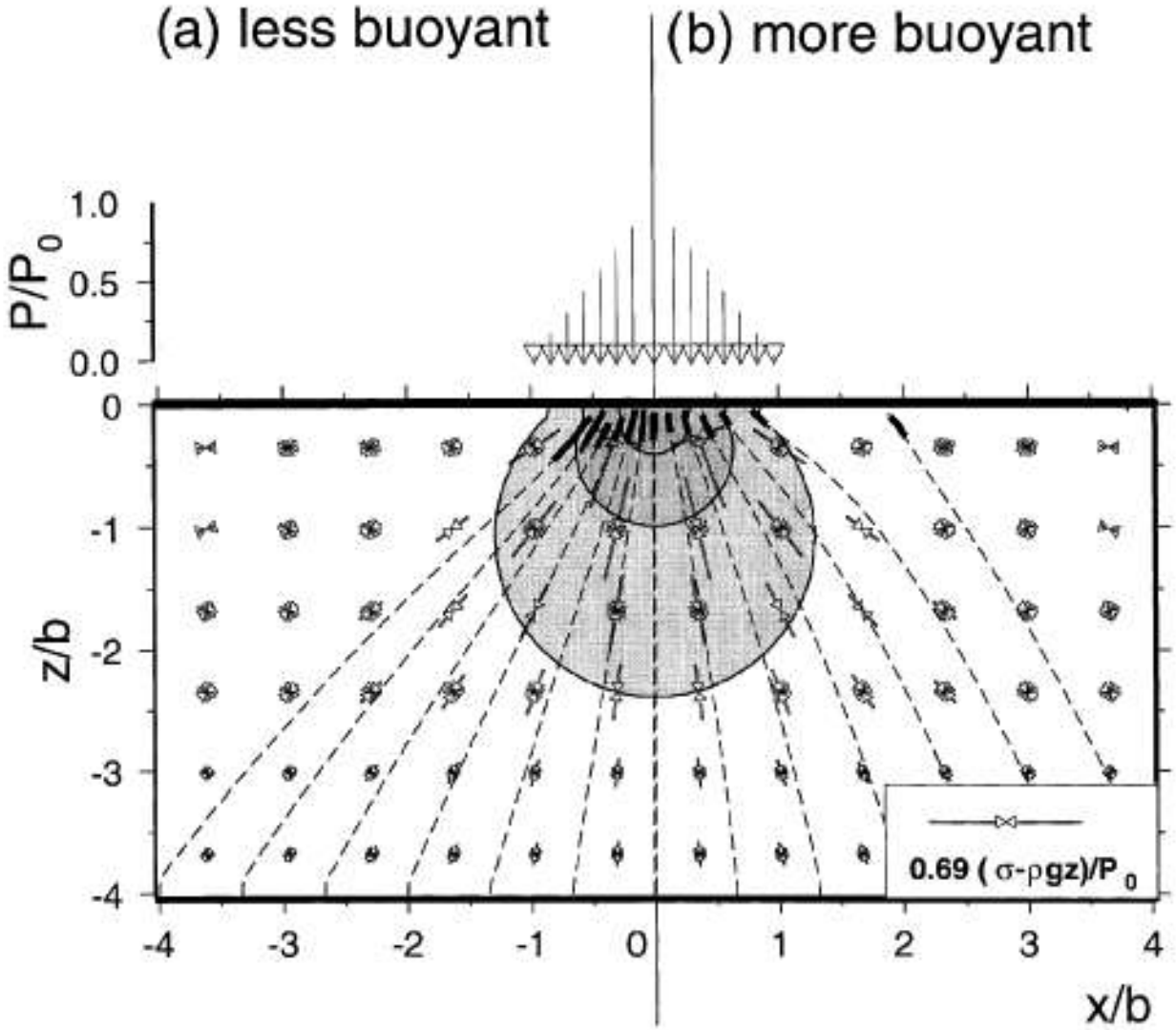

Dahm, 2000

Loading due to a volcanic edifice

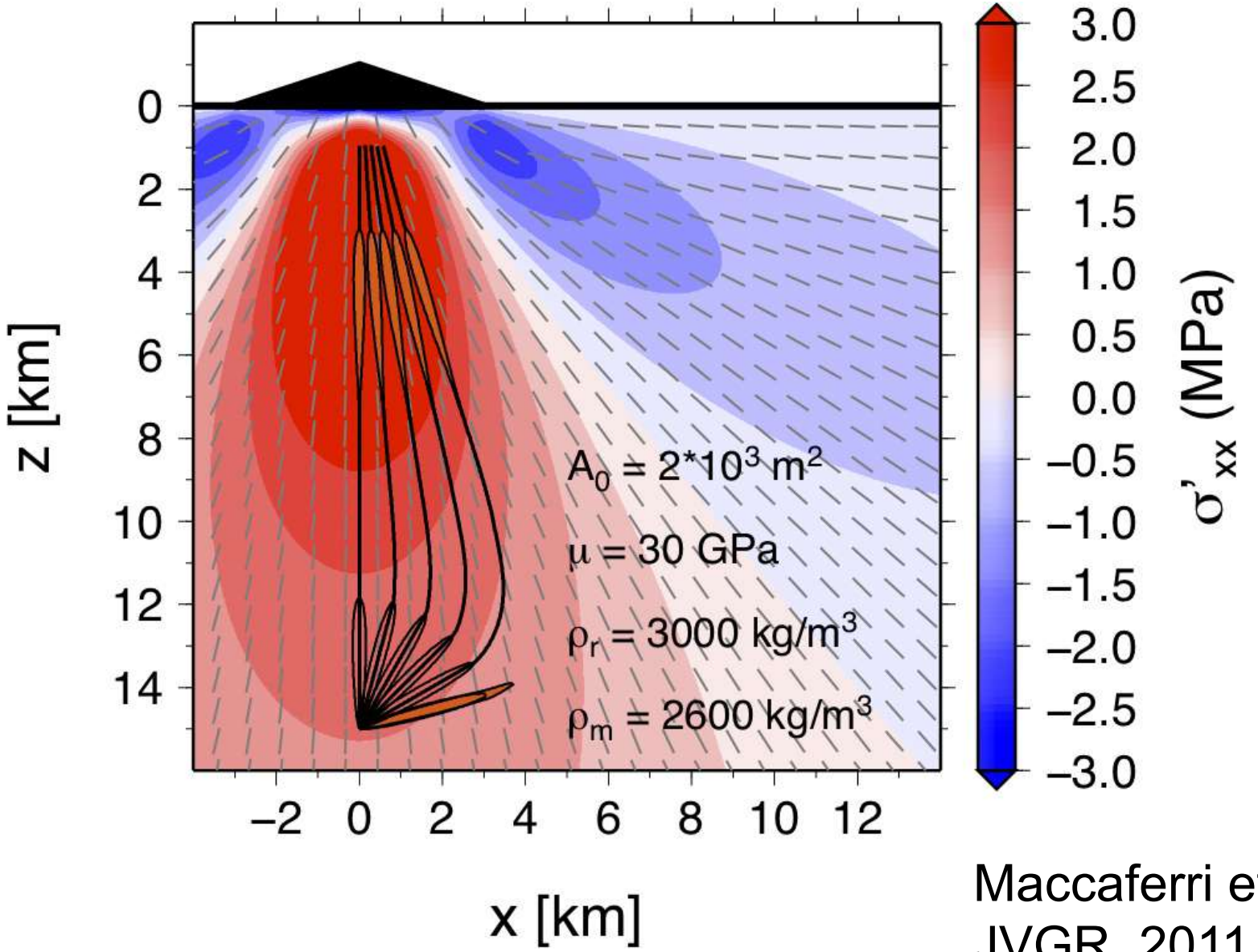

Maccaferri et al., JVGR, 2011

Loading due to a volcanic edifice

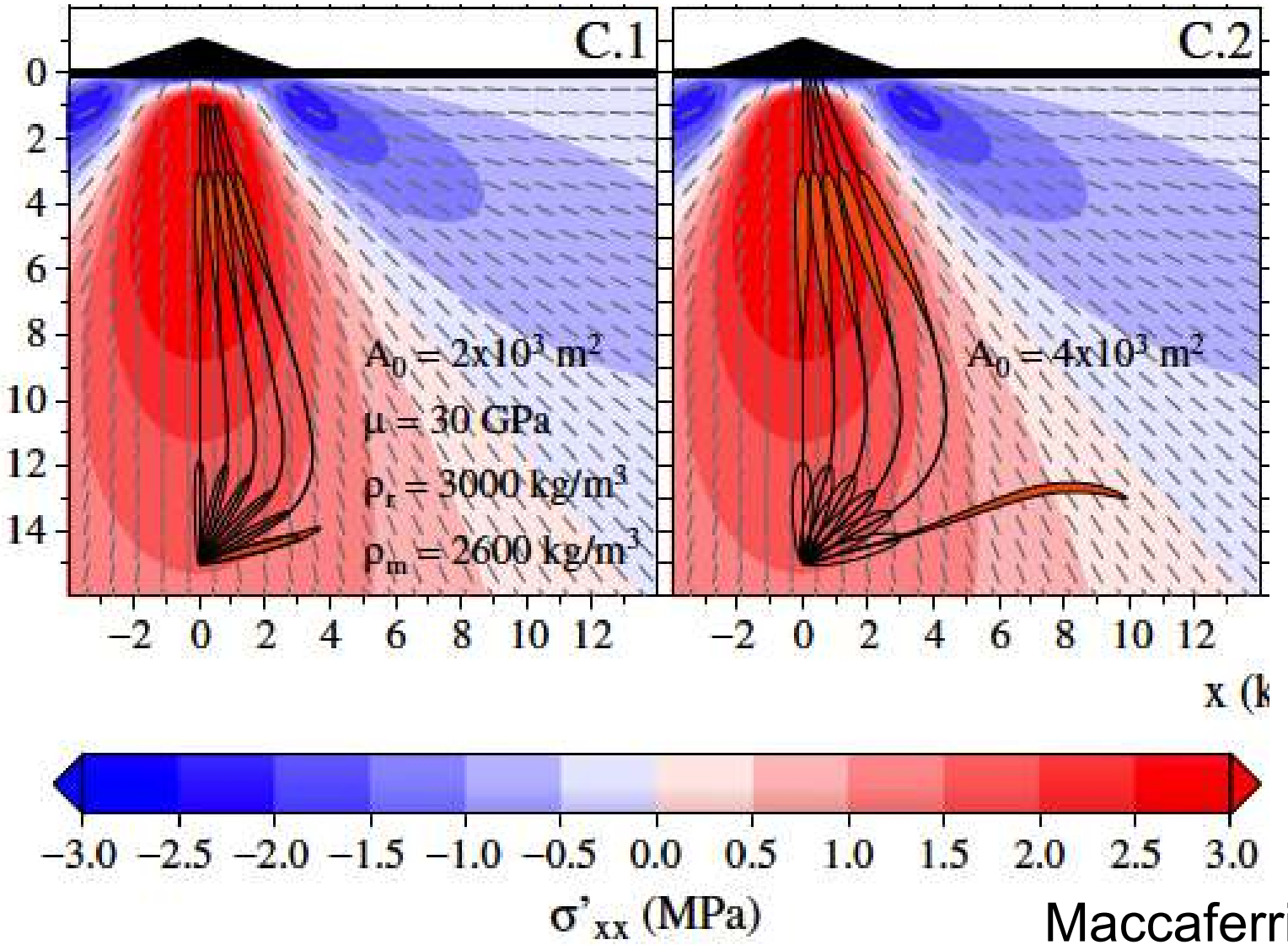

Maccaferri et al., JVGR, 2011

Boundary element modeling of dike propagation

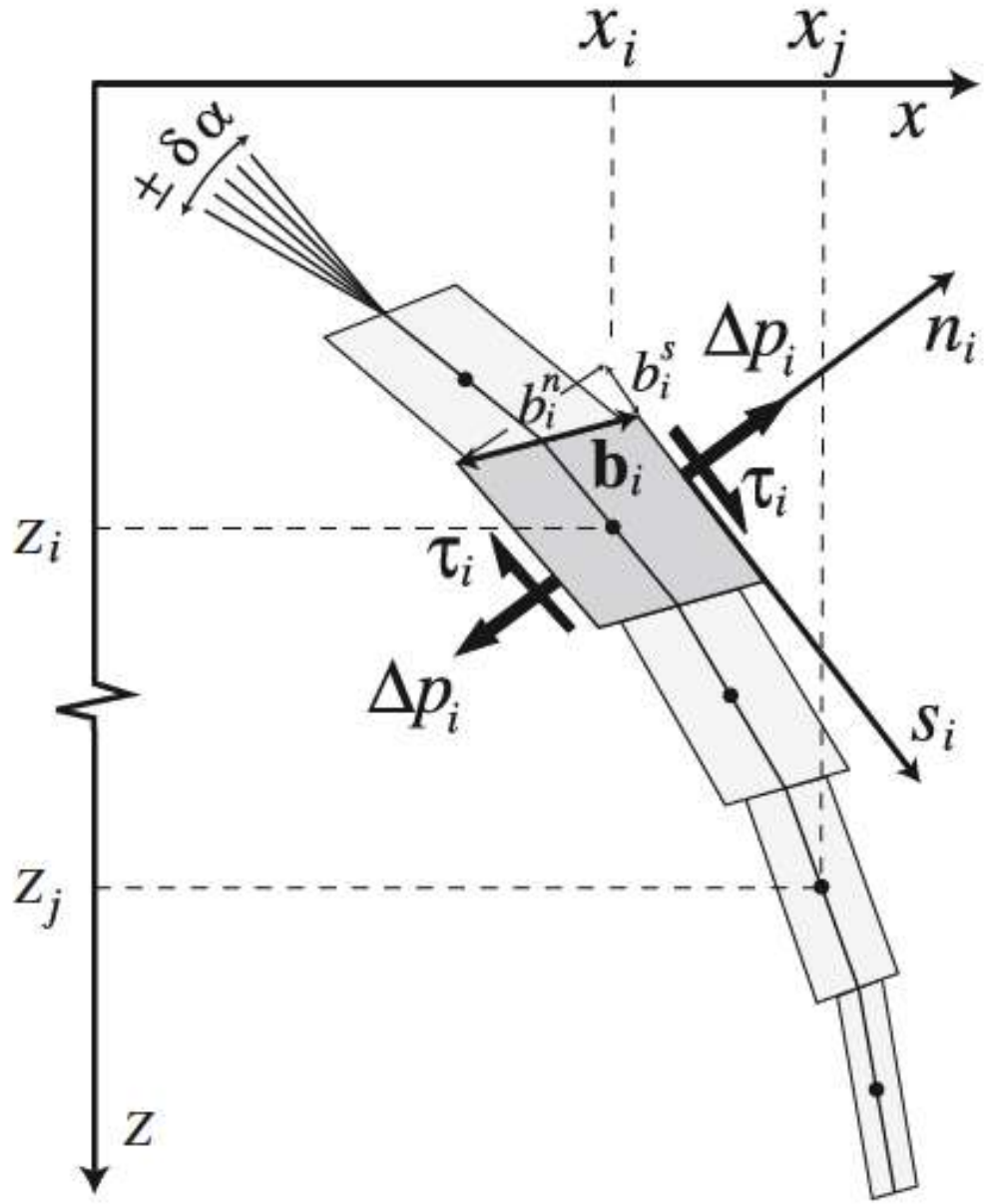

Maccaferri et al., JVGR, 2011

Methods:
Analog experiments

Homogeneous medium

High to low stiffness

High to low stiffness (rotten)

Low to high stiffness

Low to high stiffness

Low to high stiffness

Low to high stiffness

Rivalta et al., 2005,

Rivalta and Dahm, 2006

Loading due to a volcanic edifice

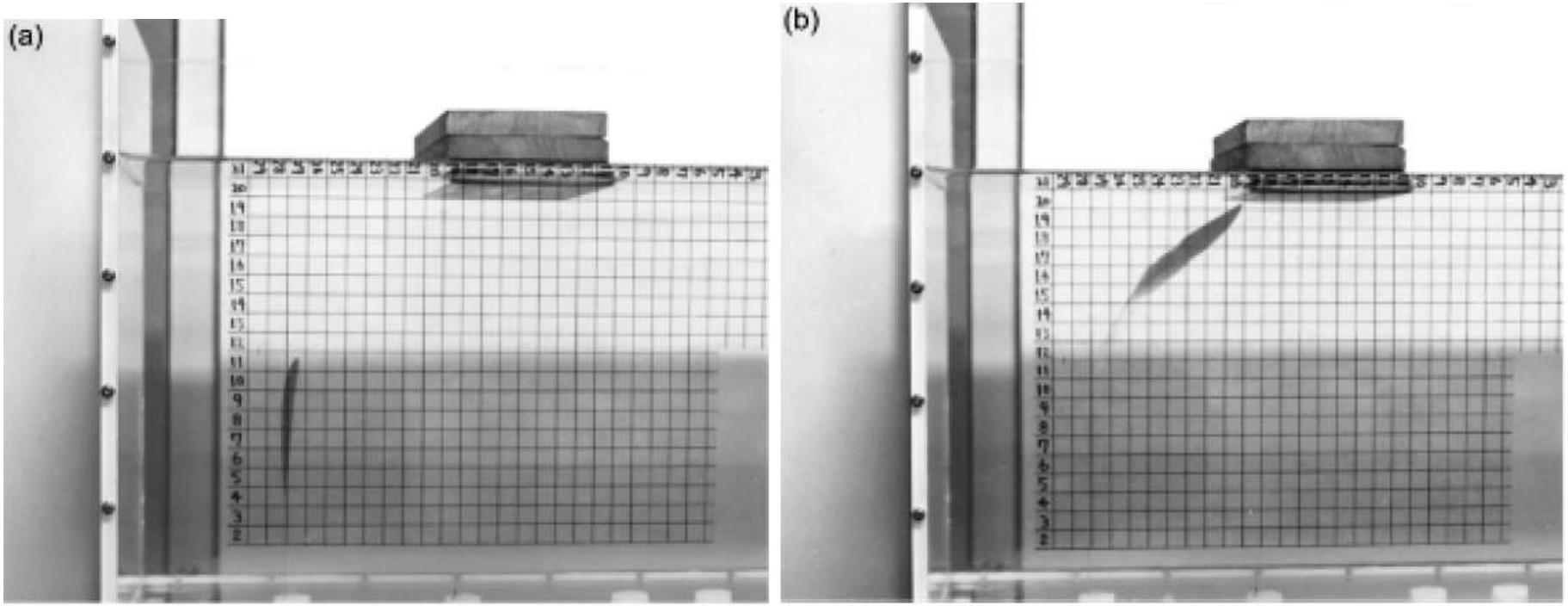

Watanabe et al., 2002

Unloading due to icecap melting

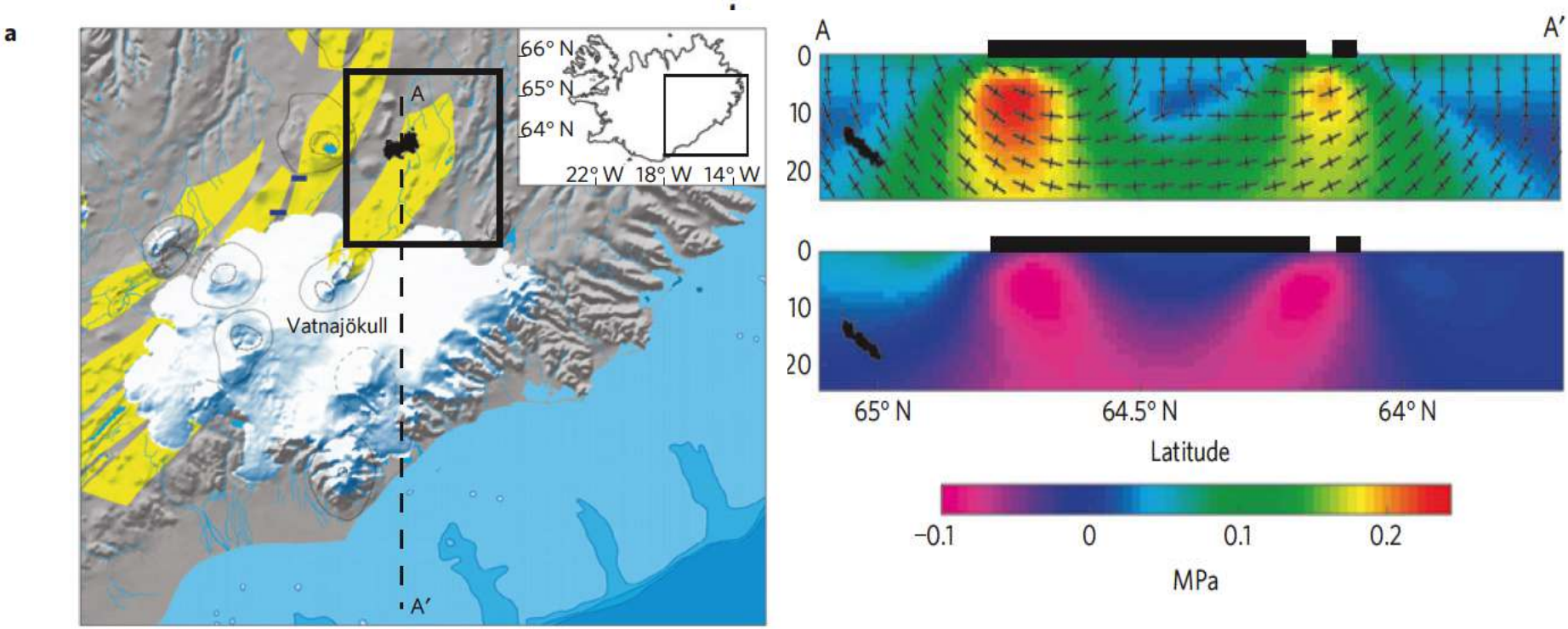

Hooper et al., 2010

Unloading due to caldera collapse

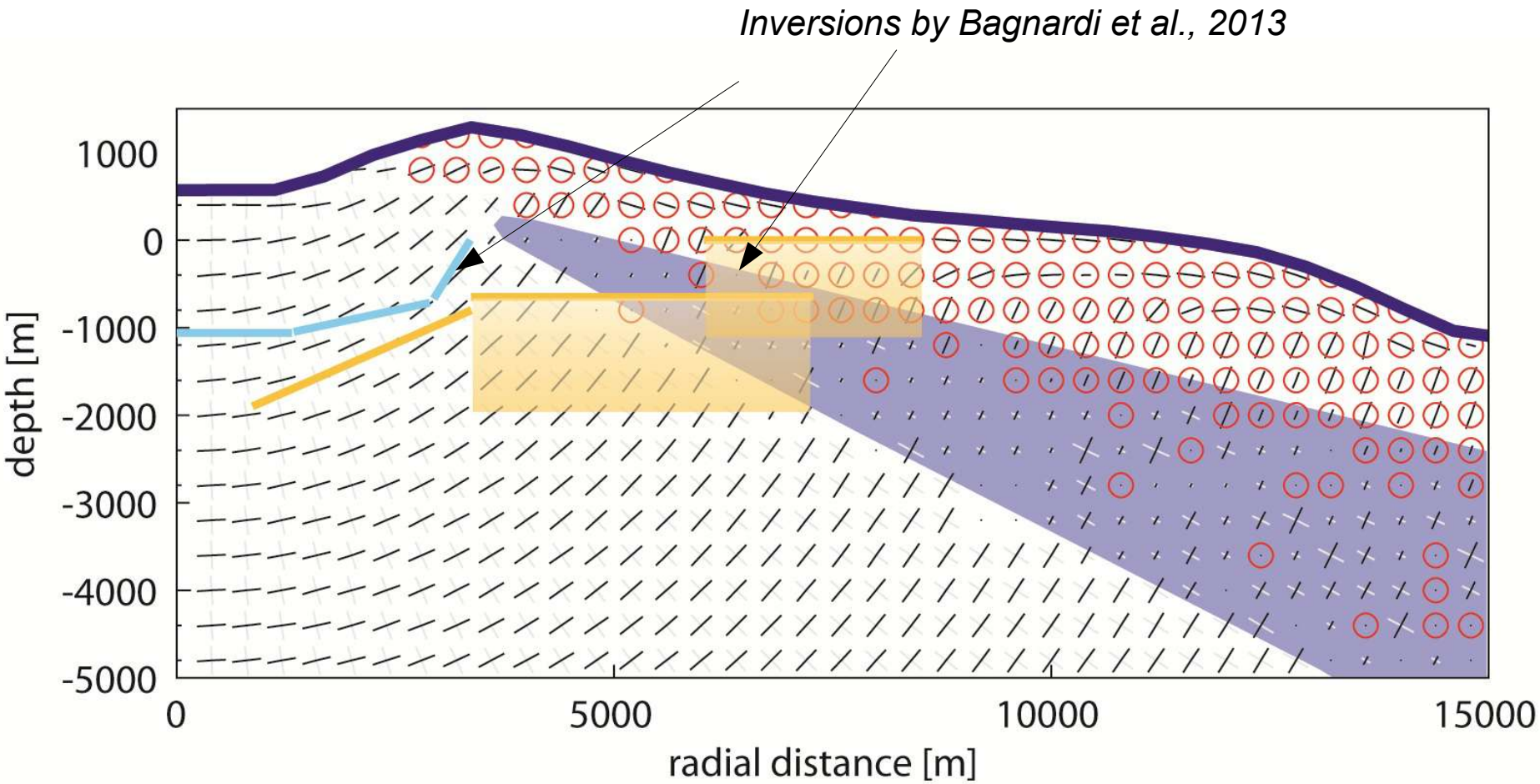

Corbi et al., 2015

Unloading due to caldera collapse

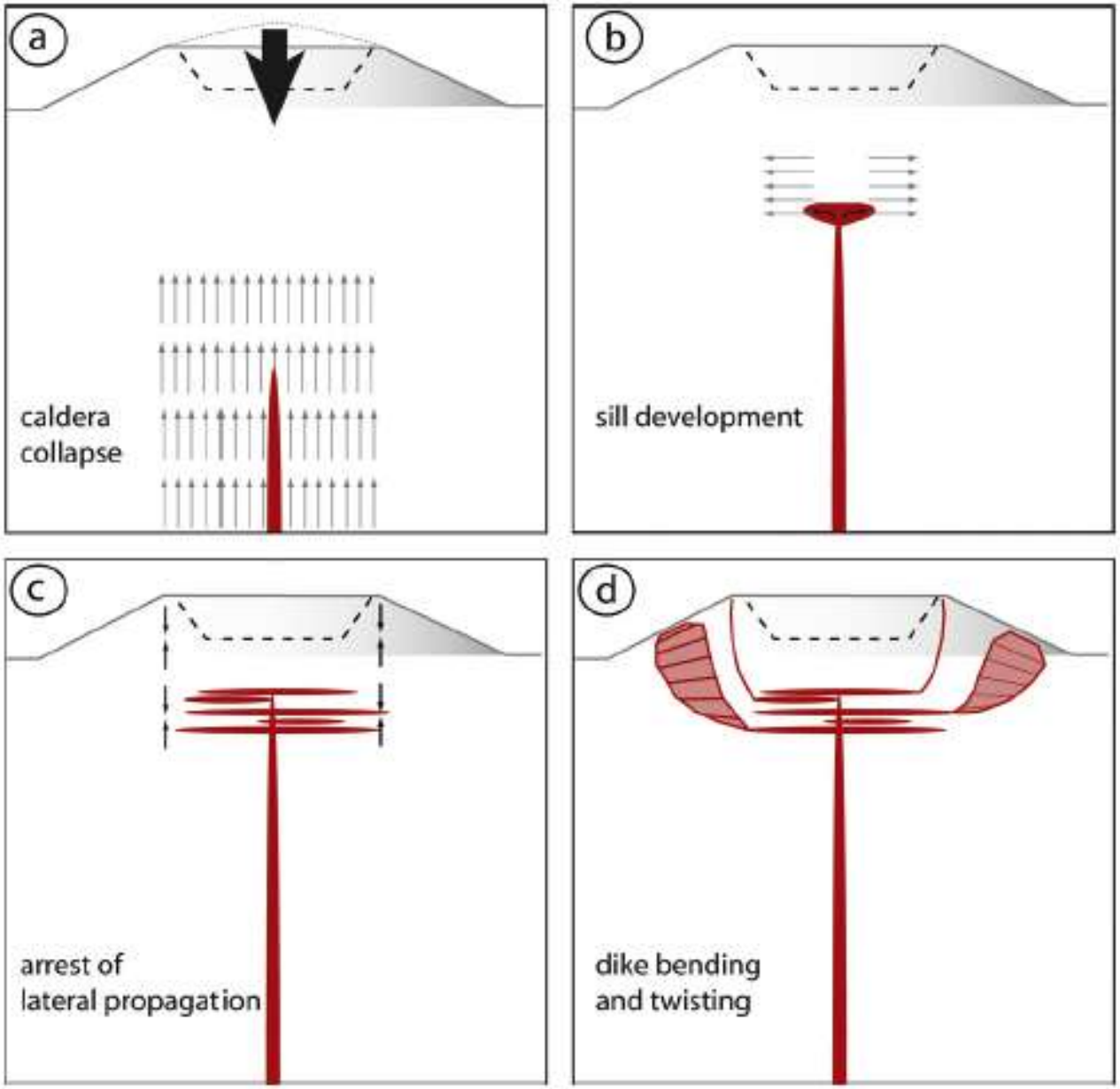

Corbi et al., 2015

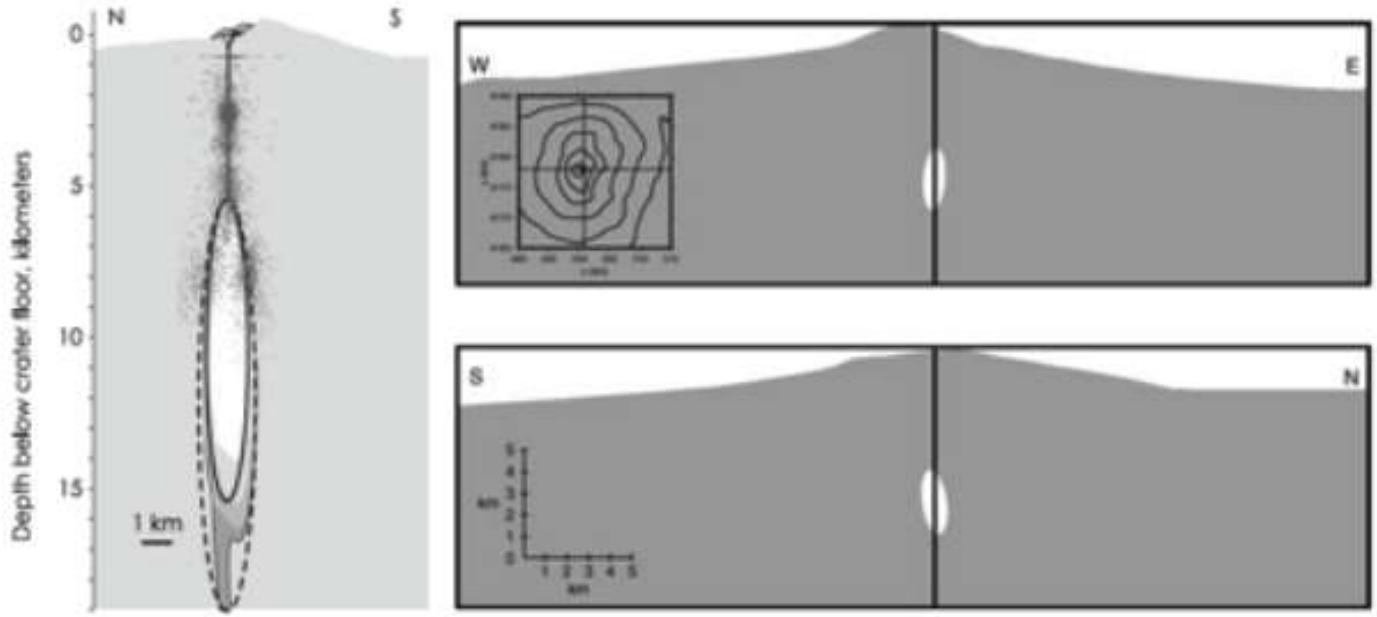

Fig. 6: Proposed models of magma chamber shape for stratovolcanoes: left) Mt. S. Helen, USA (from Mastin et al., 2009) and right) Etna, Italy (Bonaccorso et al., 2005)

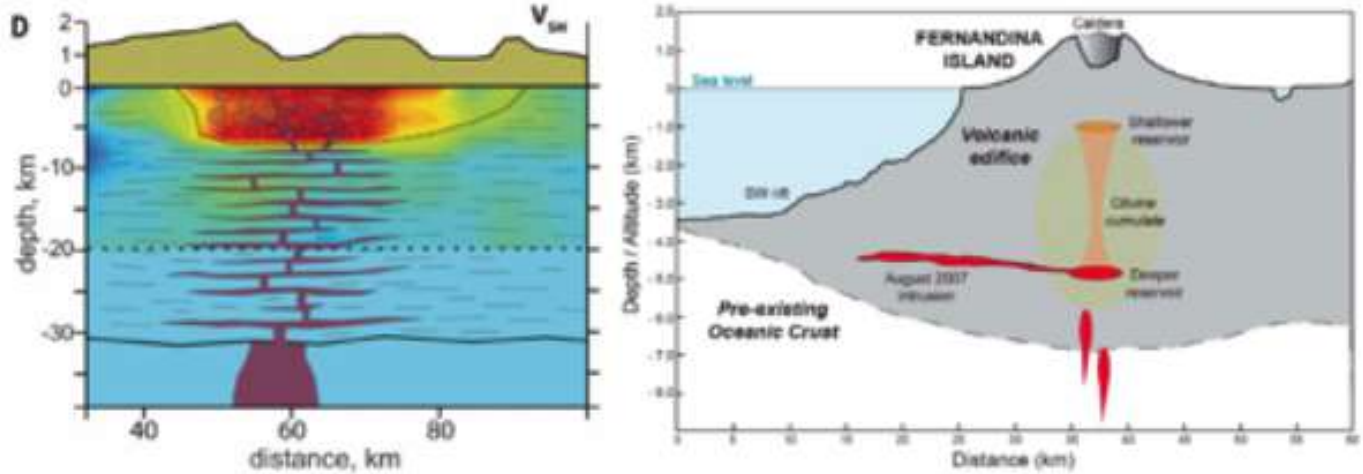

Fig. 7: Proposed models for magma reservoir arrangement for calderas: left) Toba, Sumatra (Jaxybulatov et al., 2014), right) Fernandina, Galapagos (Bagnardi et al., 2012)

Intersecting dikes

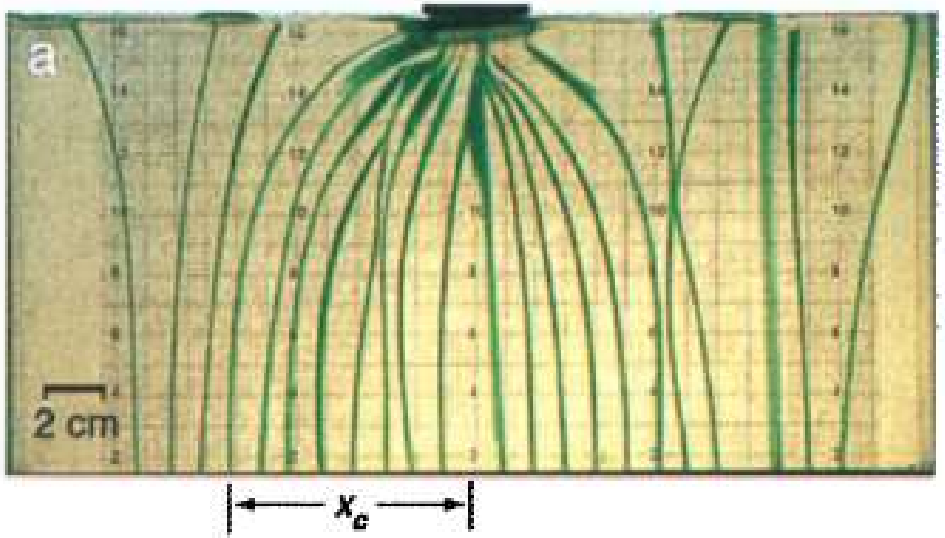

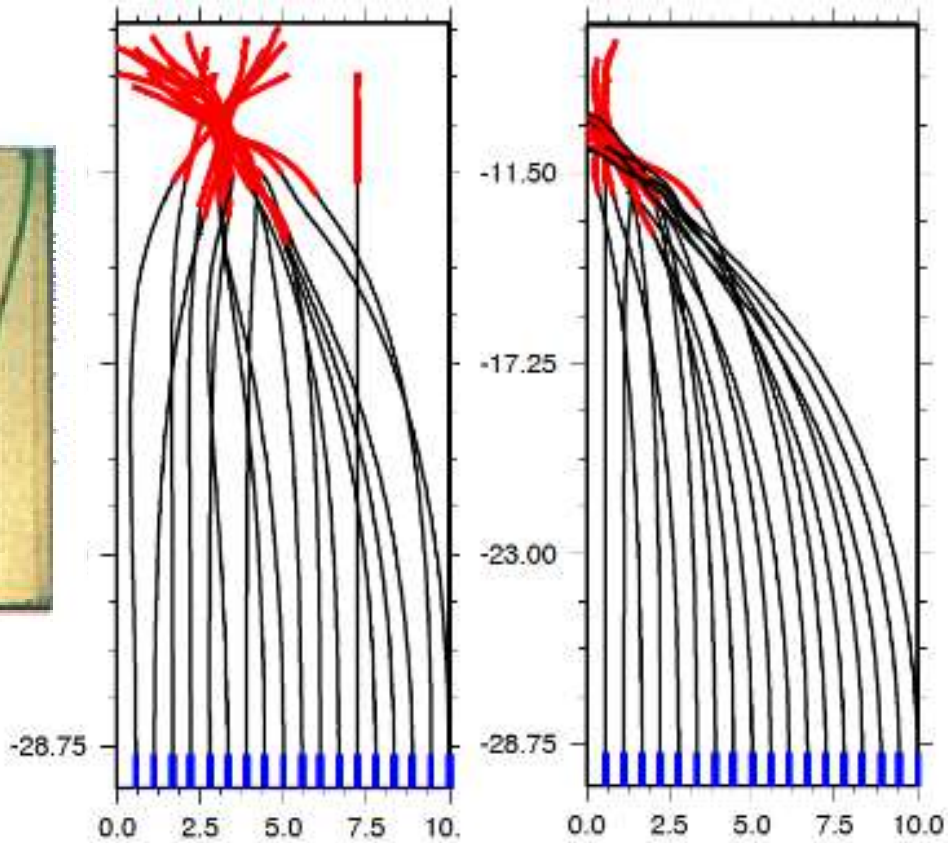

Desert rose

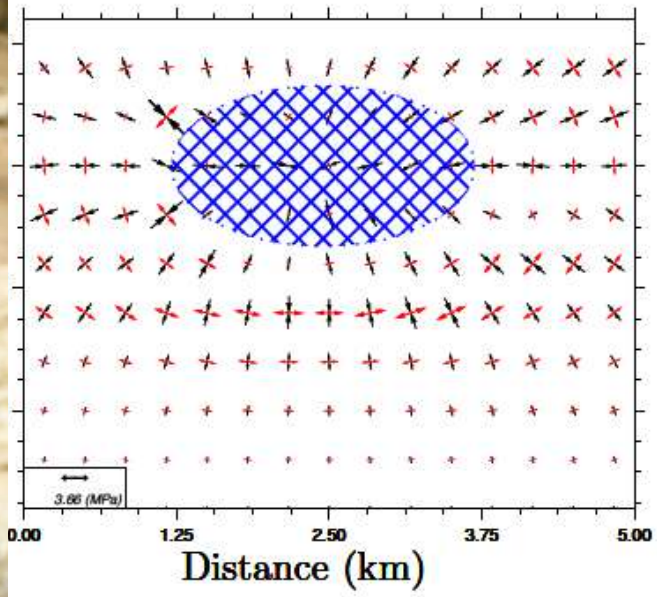

Stratovolcano

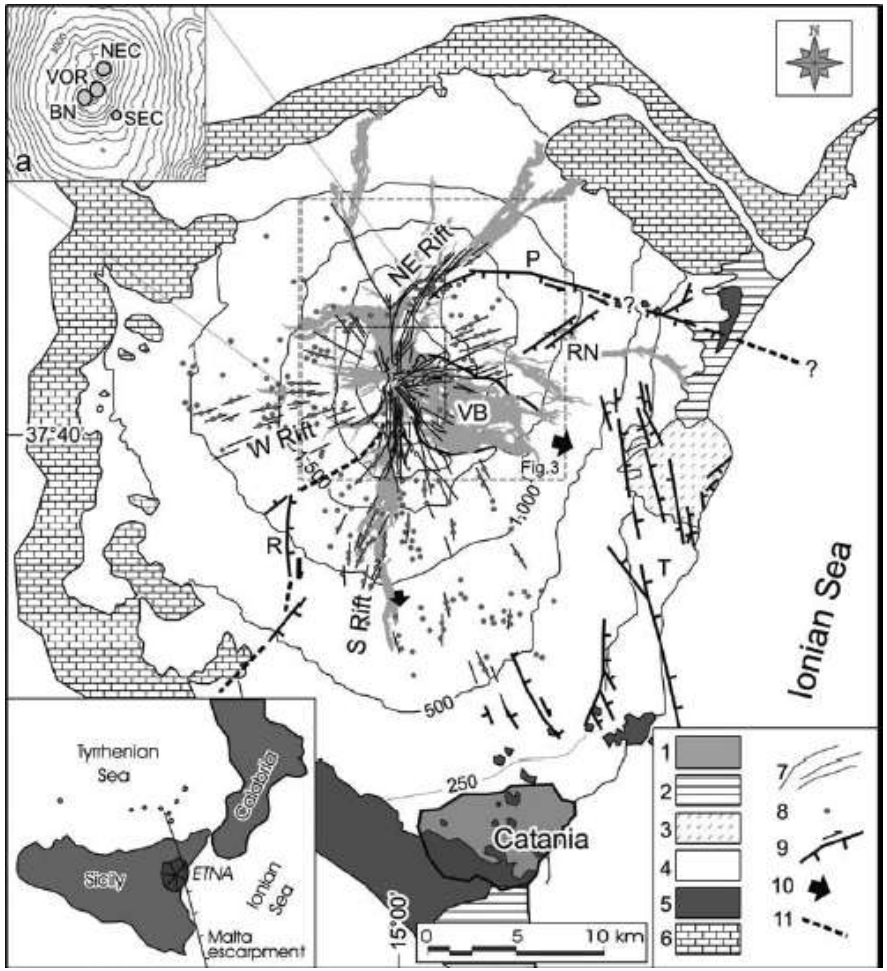

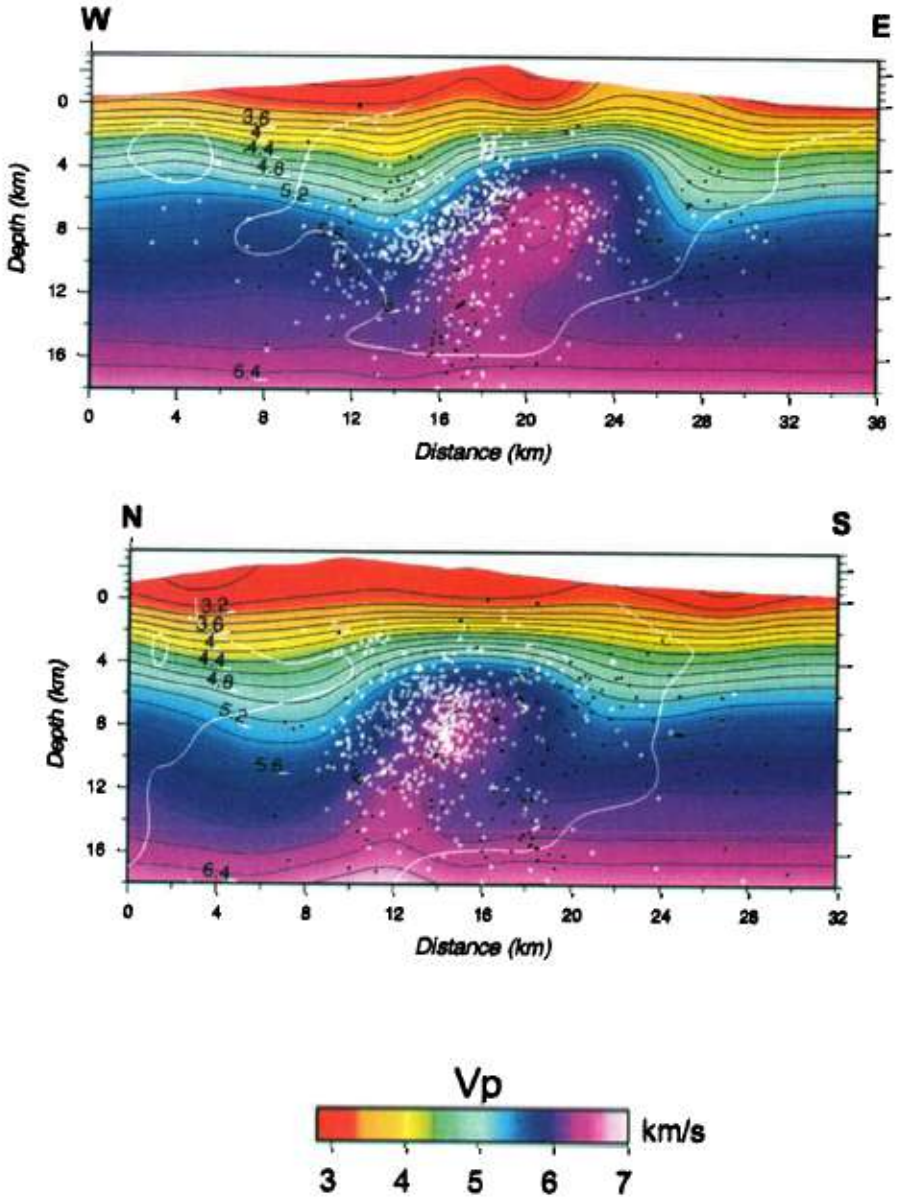

Mt. Etna, Italy *(Acocella and Neri, 2003)*

(Chiarabba et al., 2003)

Calderas

Toba caldera
(Jaxybulatov et al., 2014)

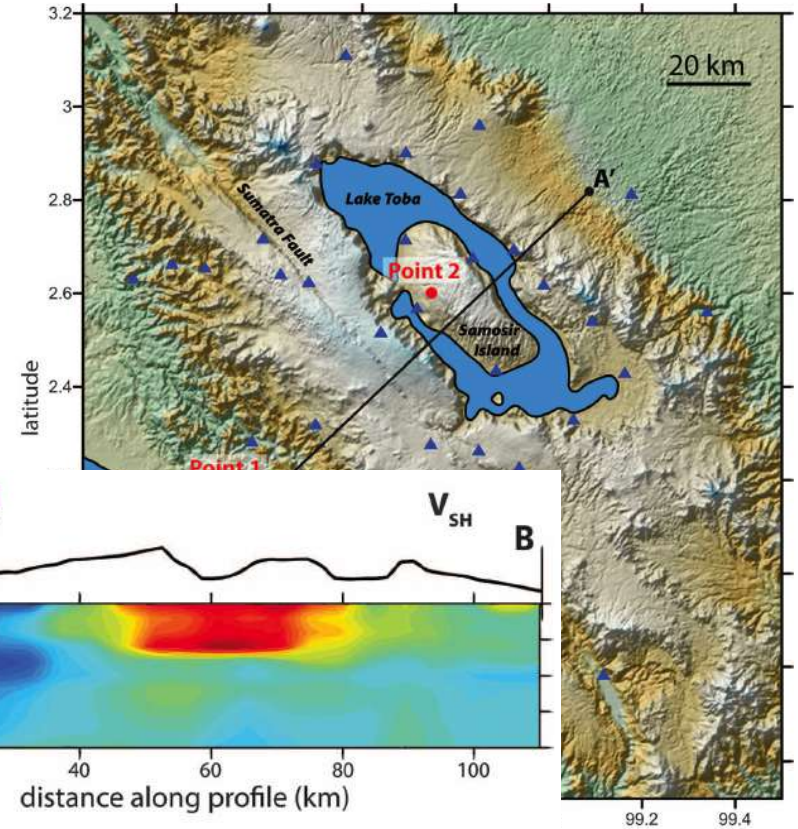

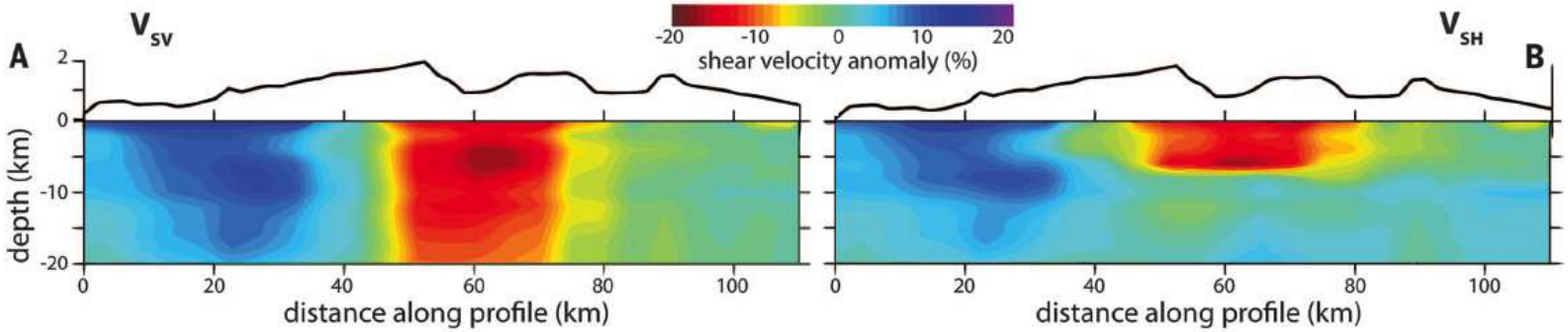

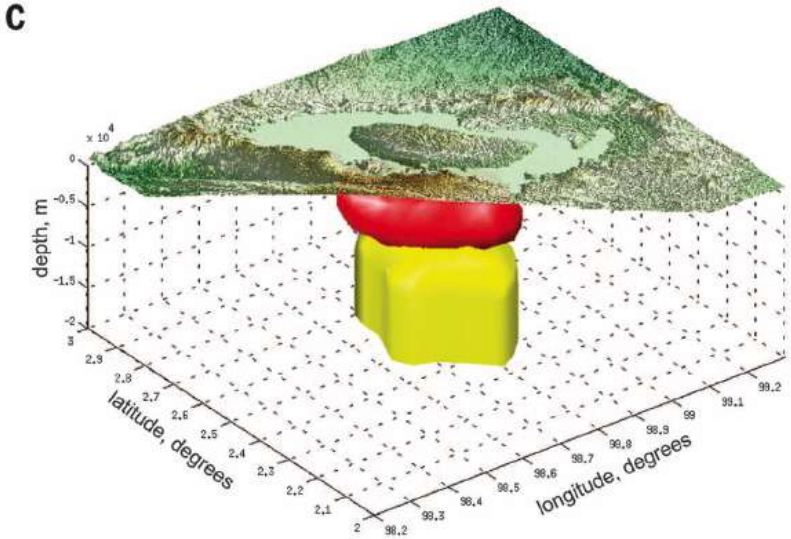

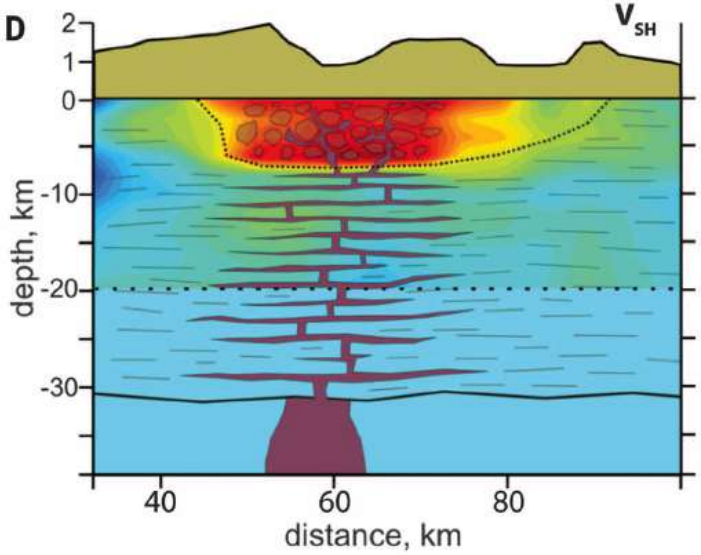

Baikal rift

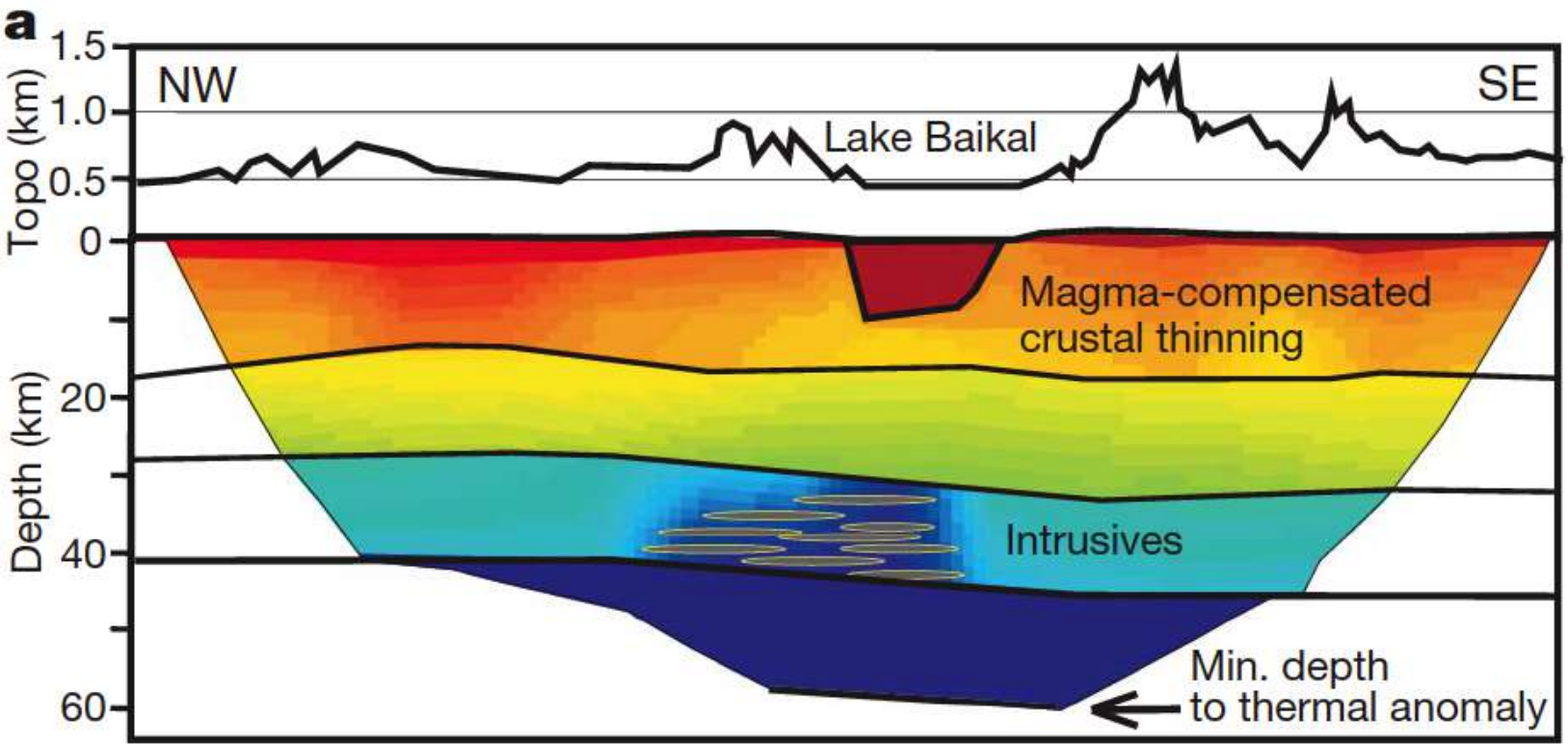

Thybo and Nielsen, Nature, 2009

Off-rift volcanism: lake Baikal

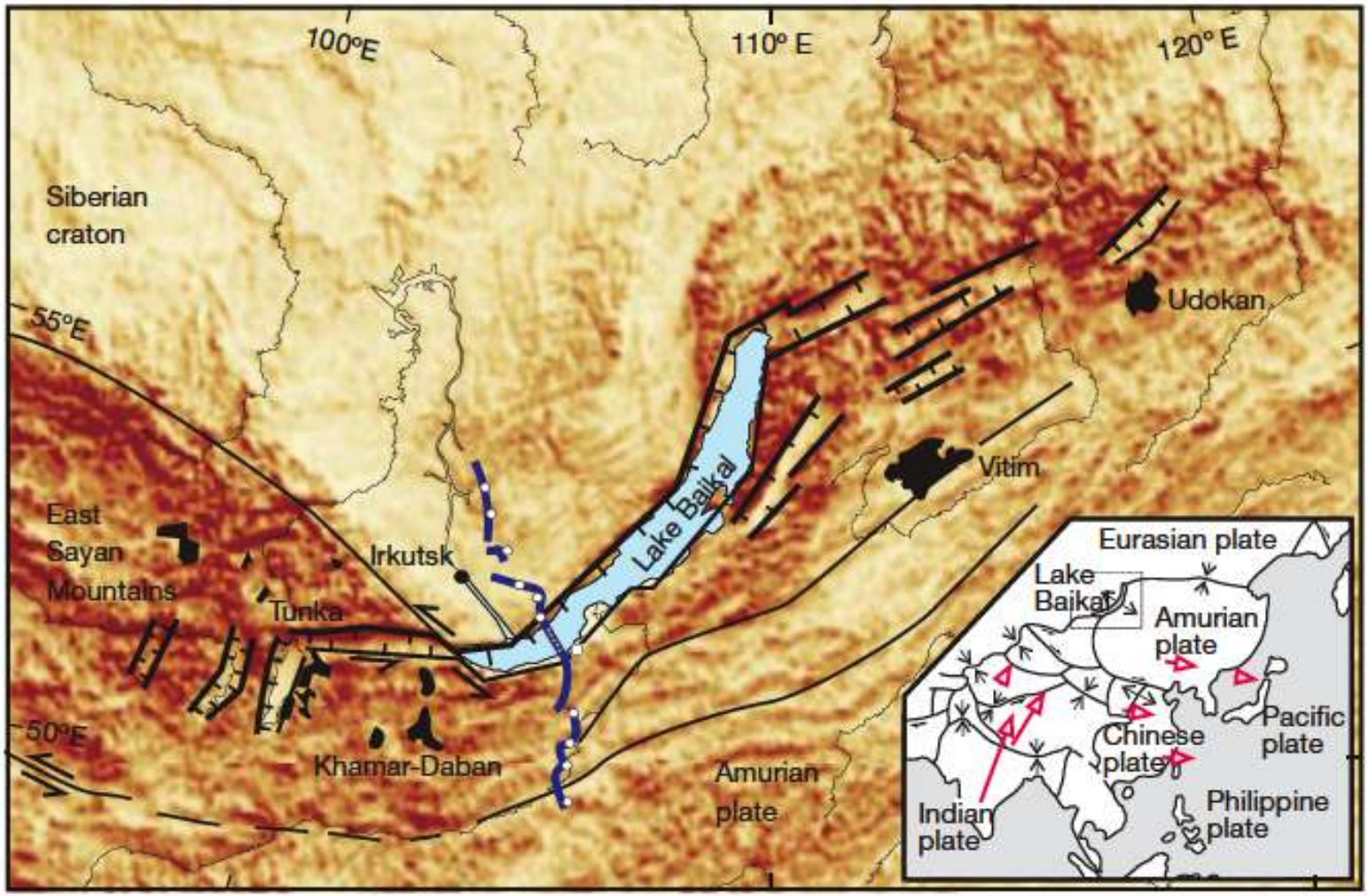

Thybo and Nielsen, Nature, 2009

Deep, narrow rifts

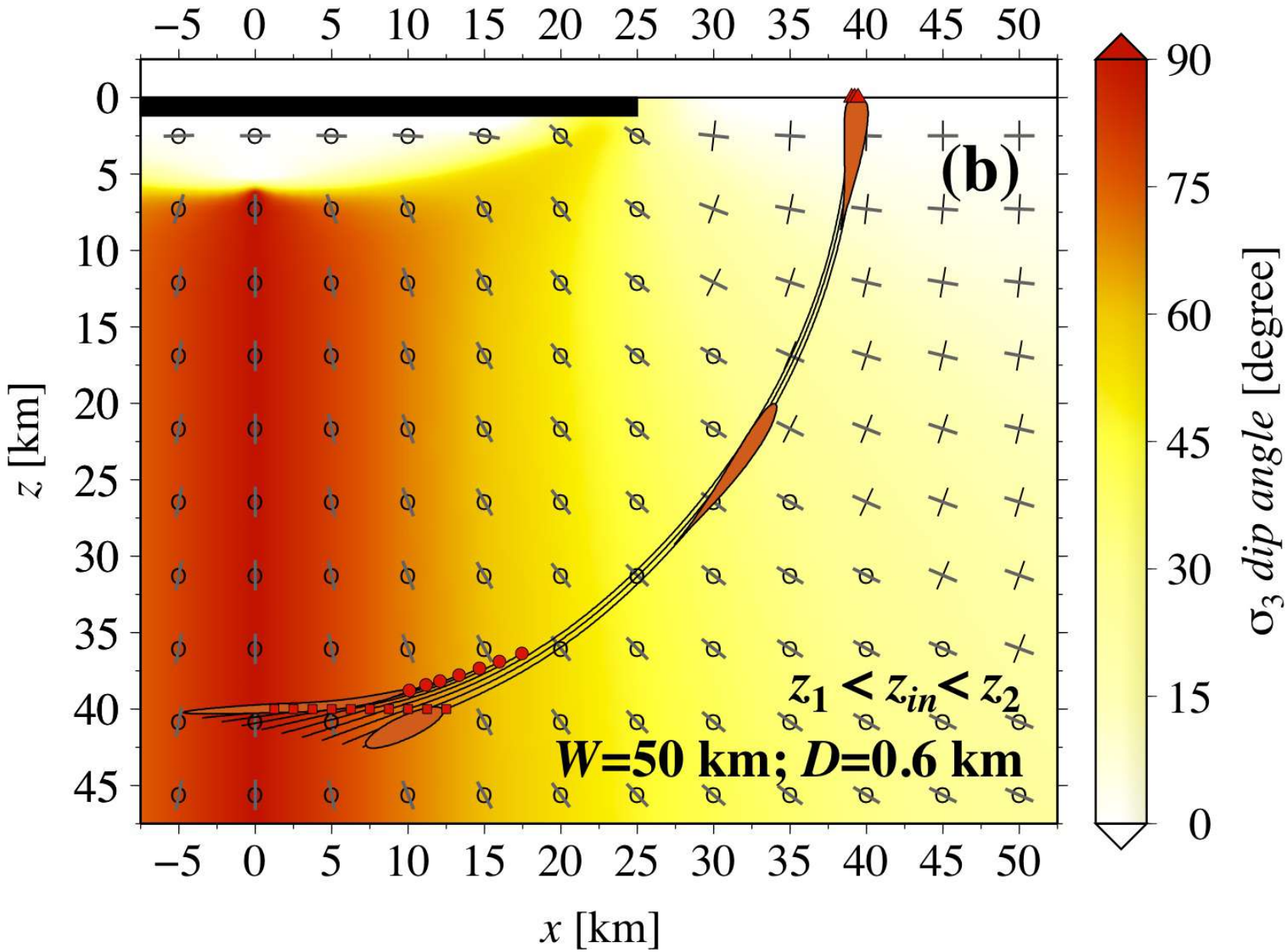

Evolution of continental rifts: final stage

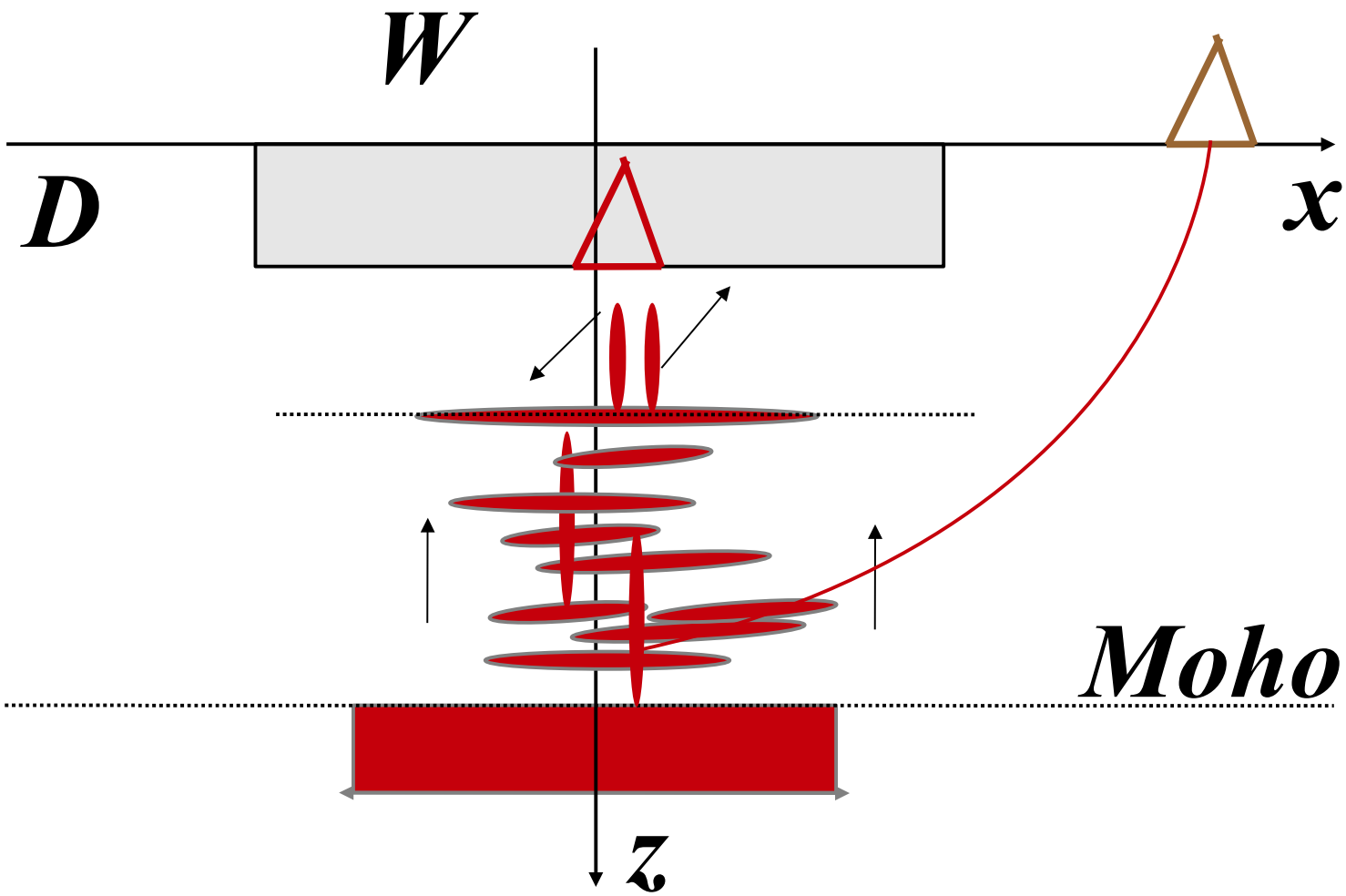

Maccaferri et al., submitted

Fault scarps

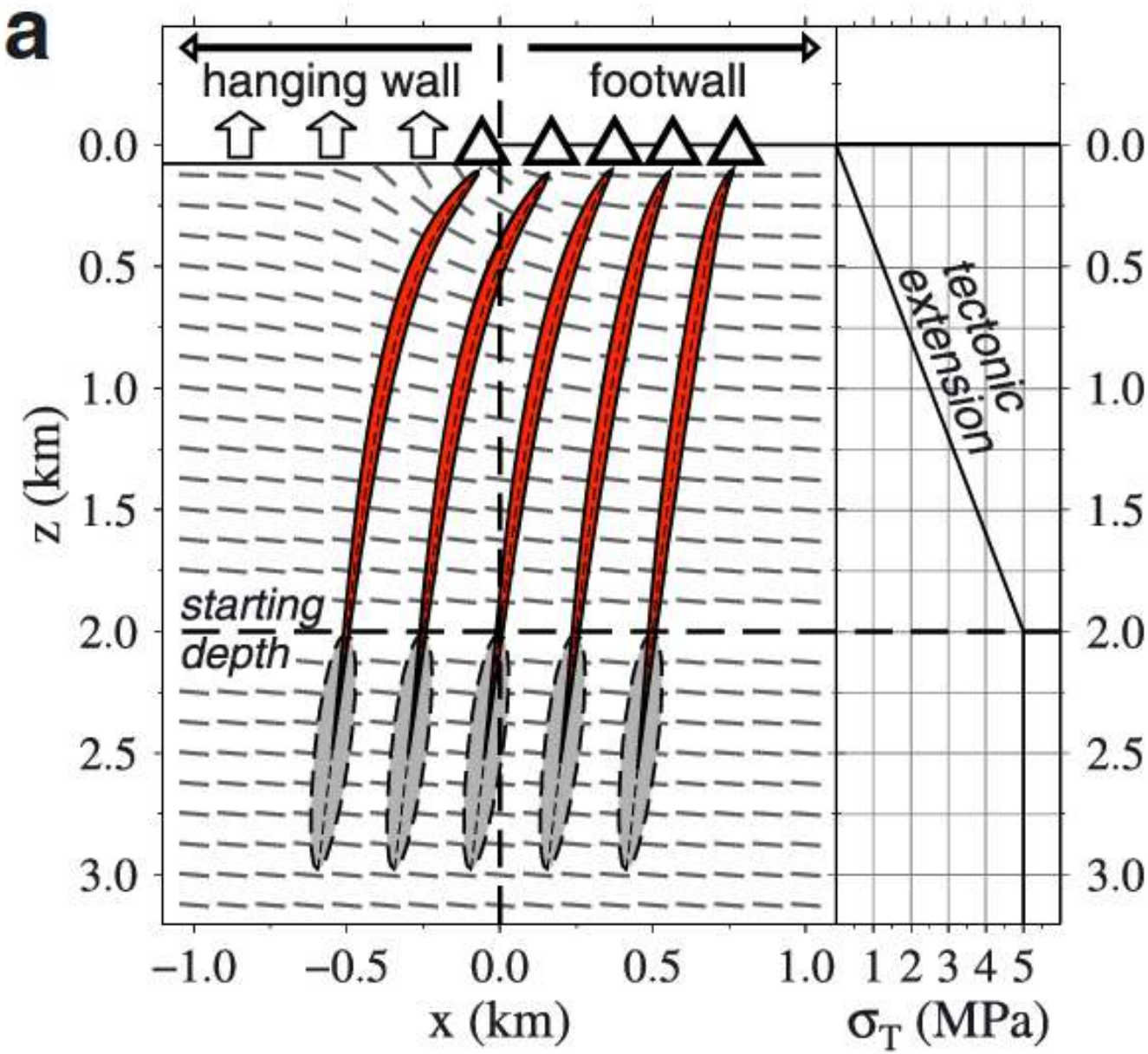

Maccaferri et al., 2015

Fault scarps

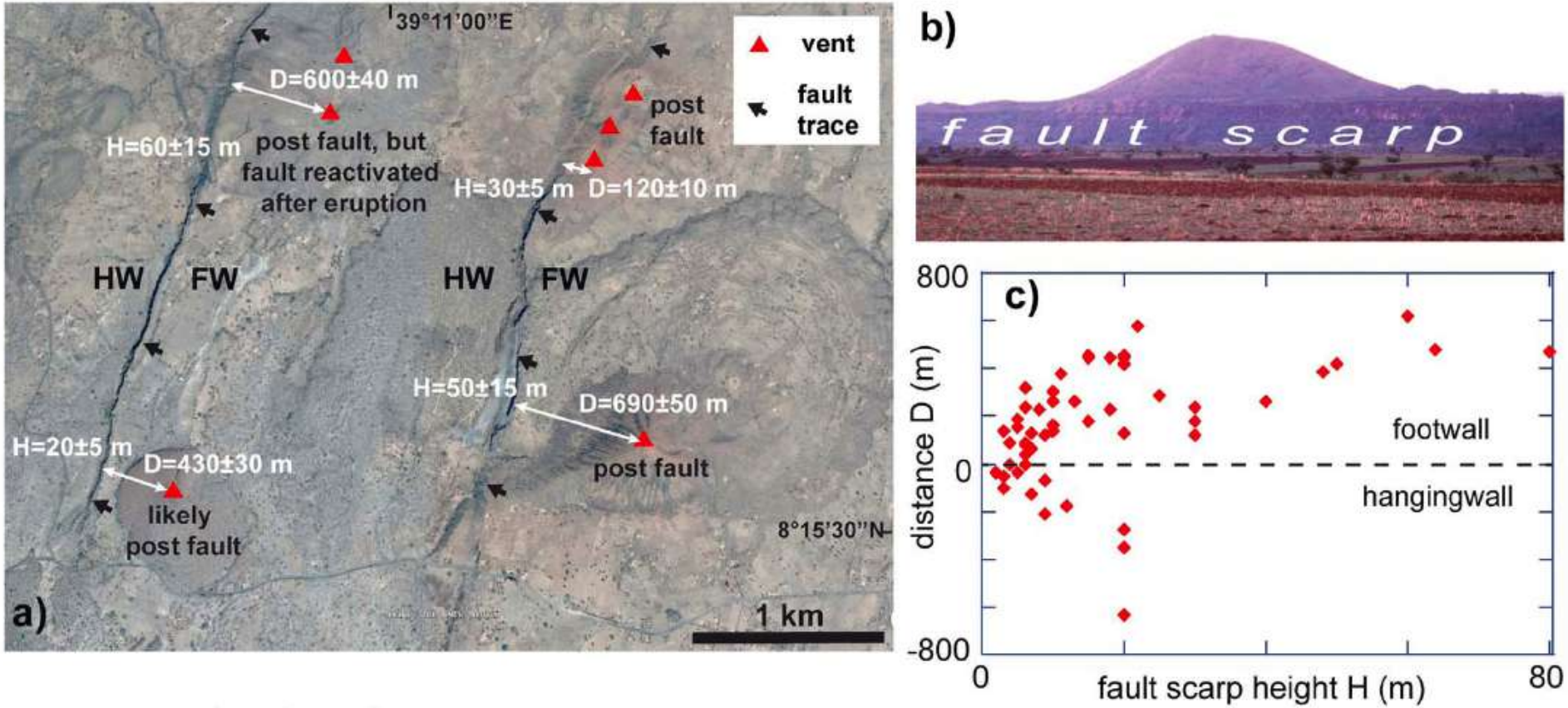

Maccaferri et al., 2015

Surface distribution of volcanoes

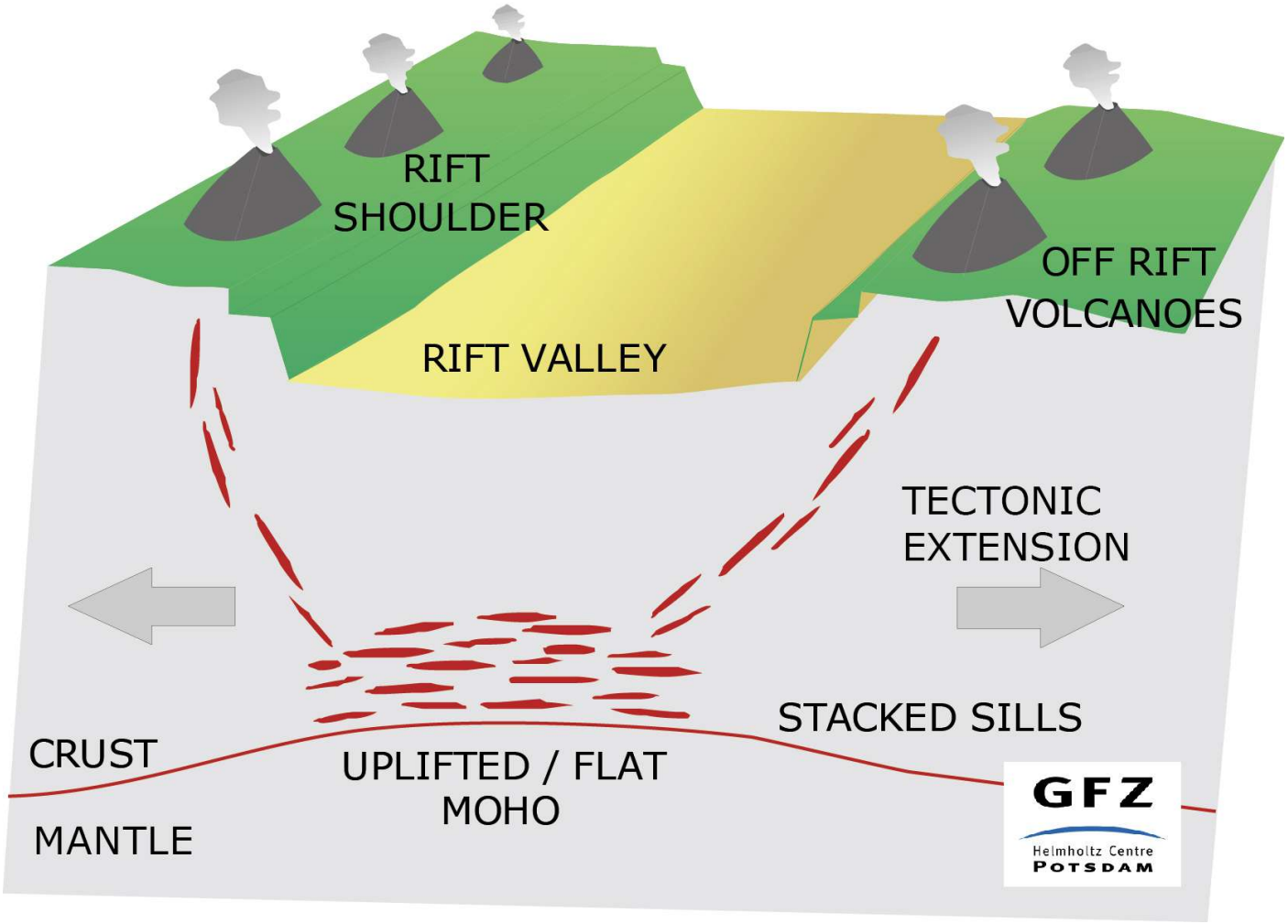

Red Sea

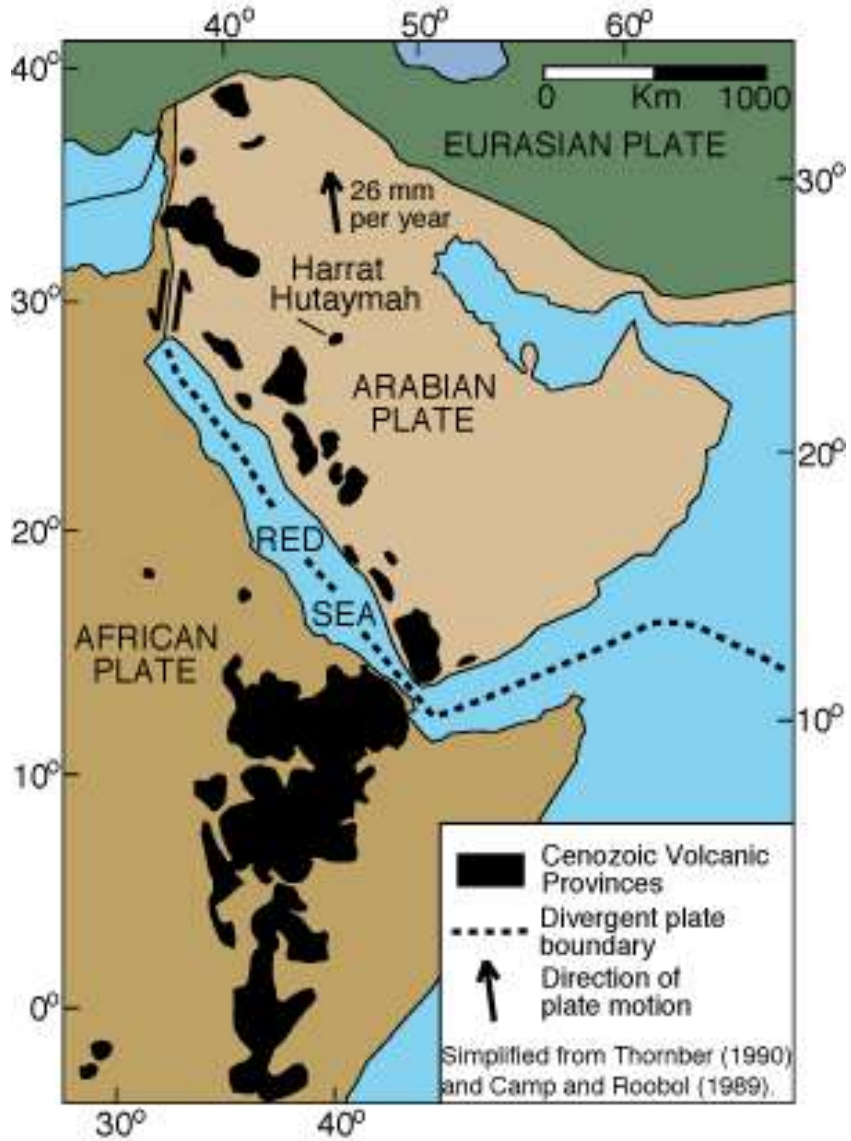
40°
50°
60°
40°
30°
20°
10°
0°
30°
40°
0
Km
1000
EURASIAN PLATE
26 mm
per year
Harrat
Hutaymah
ARABIAN
PLATE
RED
SEA
AFRICAN
PLATE
Cenozoic Volcanic
Provinces
Divergent plate
boundary
Direction of
plate motion
Simplified from Thornber (1990)
and Camp and Roobol (1989).

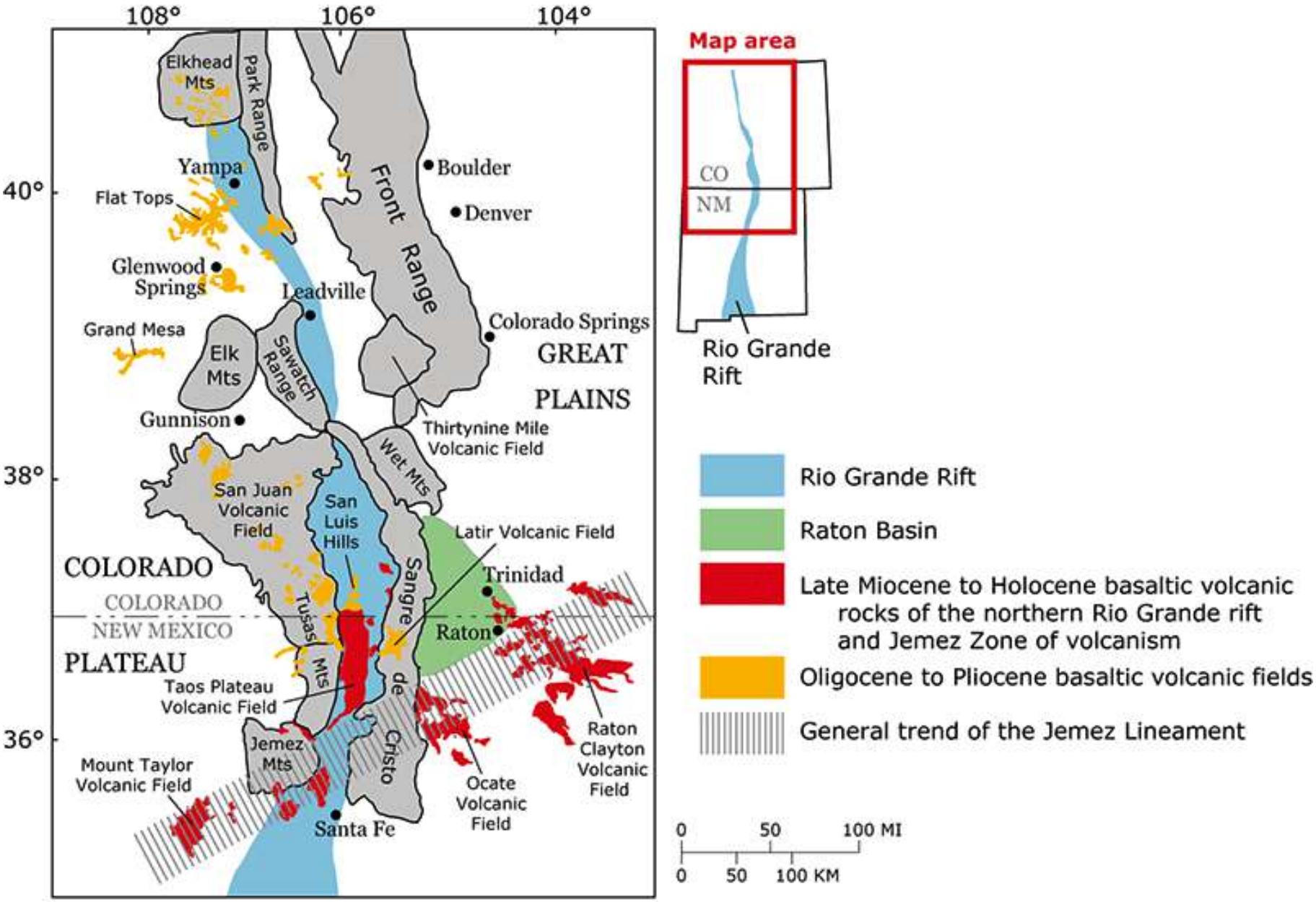
108°
106°
104°
40°
38°
36°
Elkhead Mts
Park Range
Yampa
Flat Tops
Glenwood Springs
Grand Mesa
Elk Mts
Leadville
Sawatch Range
Gunnison
Front Range
Boulder
Denver
Colorado Springs
GREAT PLAINS
Thirtynine Mile Volcanic Field
Wet Mts
San Juan Volcanic Field
San Luis Hills
Latir Volcanic Field
Trinidad
Raton
COLORADO
COLORADO
NEW MEXICO
PLATEAU
Tusas Mts
Taos Plateau Volcanic Field
Sangre de Cristo
Jemez Mts
Mount Taylor Volcanic Field
Santa Fe
Ocate Volcanic Field
Raton Clayton Volcanic Field
Map area
CO
NM
Rio Grande Rift
Rio Grande Rift
Raton Basin
Late Miocene to Holocene basaltic volcanic rocks of the northern Rio Grande rift and Jemez Zone of volcanism
Oligocene to Pliocene basaltic volcanic fields
General trend of the Jemez Lineament
0 50 100 MI
0 50 100 KM

Wide, shallow rifts (z_1 is deep)

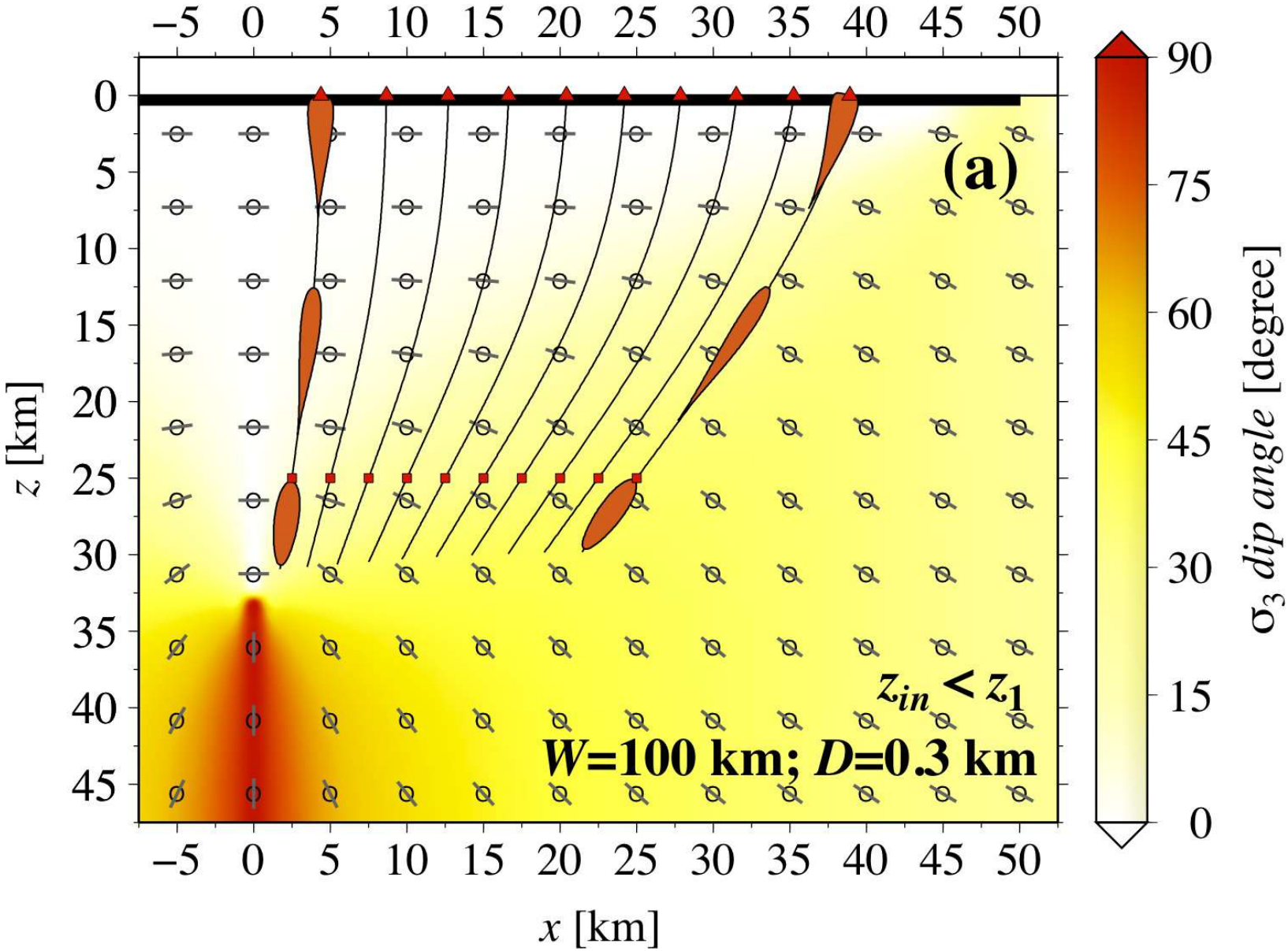

Conclusions

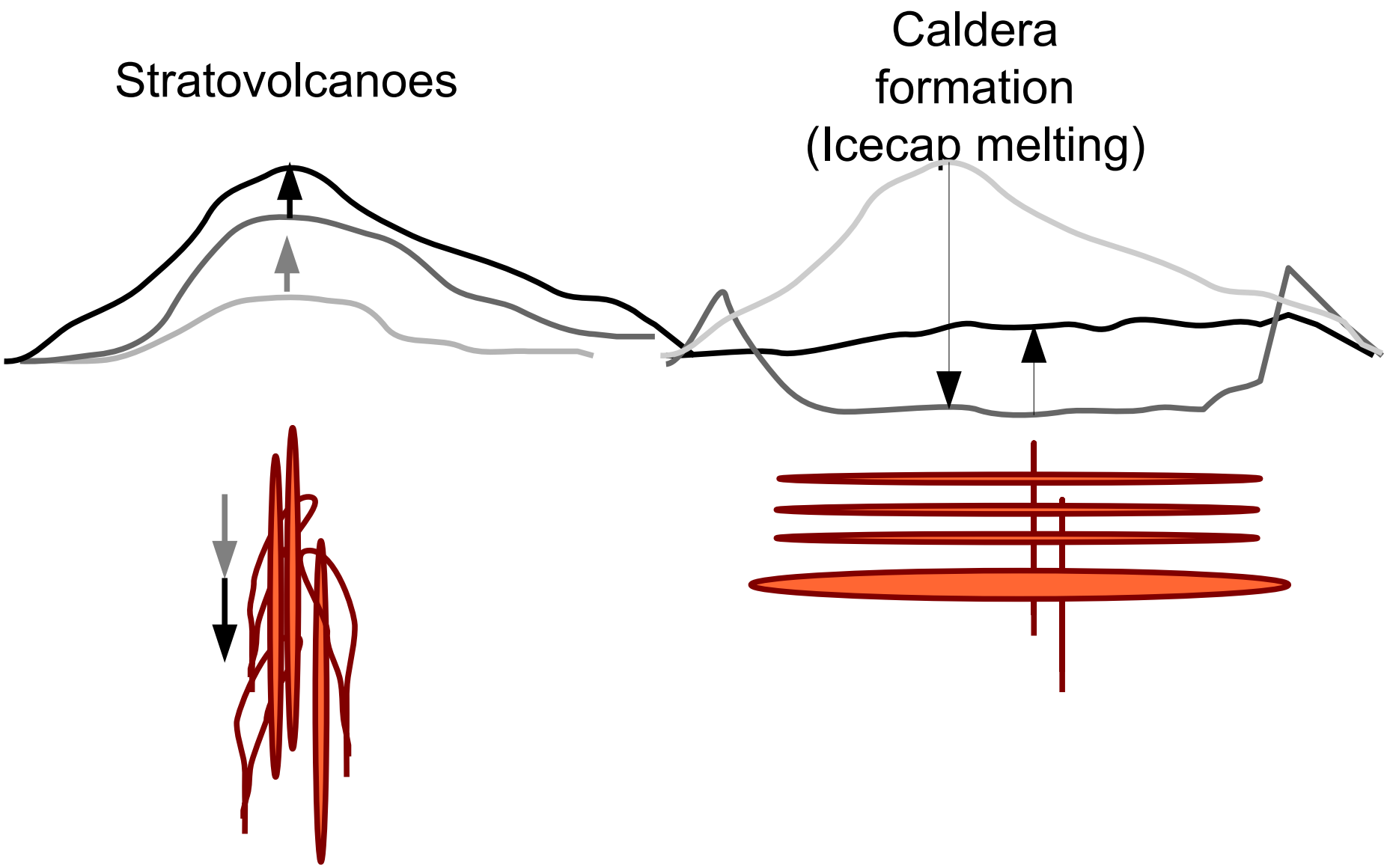

Magma storage model

$$dM = \rho\, dV + V\, d\rho = \left(\rho \frac{dV}{dp} + V \frac{d\rho}{dp}\right) dp = \rho\, V \left(\beta_e + \beta_m\right) dp$$

Magma compressibility:

$$\beta_m = \frac{1}{\rho} \frac{d\rho}{dp}$$

$$\beta_m = 10^{-11} - 10^{-10}\, Pa^{-1}$$

(or much higher if magma contains bubbles)

Source compliance:

$$\beta_e = \frac{1}{V} \frac{dV}{dp}$$

$$\beta_e(\textit{spherical chamber}) = \frac{3}{4\mu} \sim 10^{-11} - 10^{-10}\, Pa^{-1}$$

$$\beta_e(\textit{penny shaped crack}) = \frac{1}{p^i - \sigma} \sim 10^{-7}\, Pa^{-1}$$

Segall et al., 2001, Rivalta and Segall, 2008, Rivalta, 2010, Segall, 2013

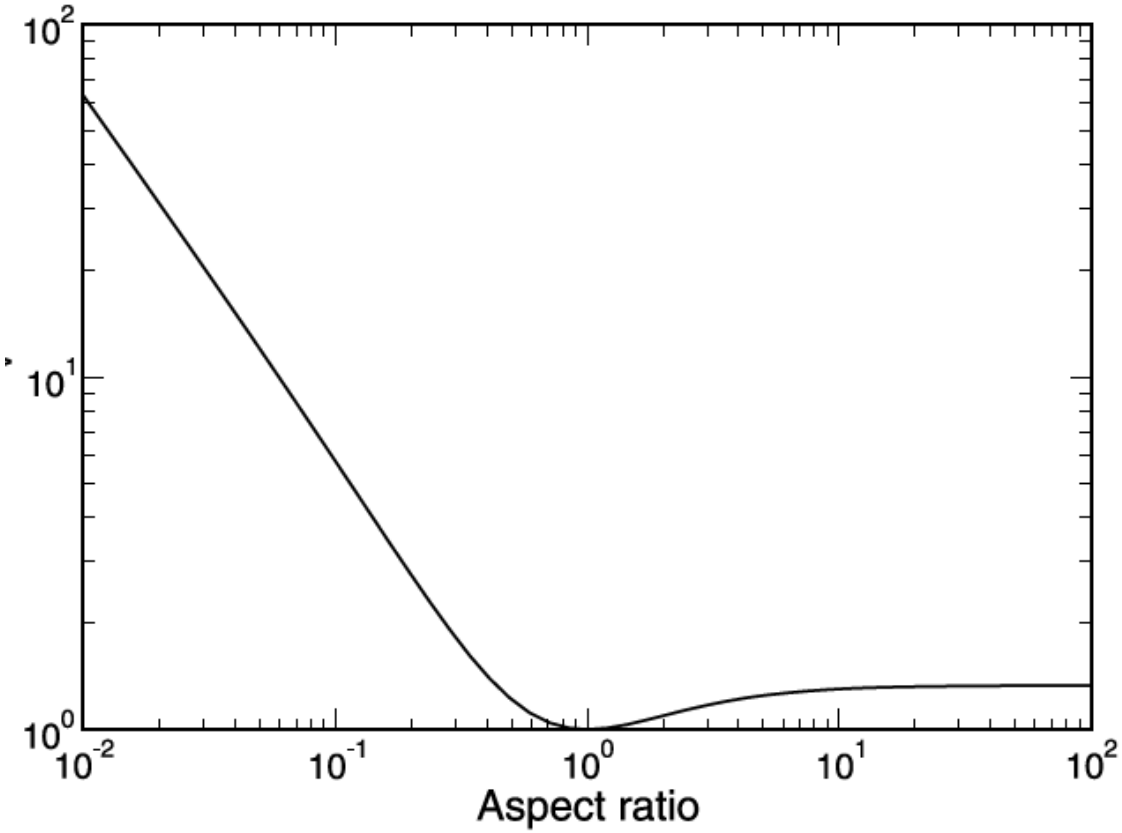

Figure 2. Ratio R_V of the volume change for a spheroidal cavity to the volume change for a spherical cavity, as a function of the aspect ratio (ratio of polar to equatorial radii) of the spheroidal cavity; $\nu = 0.25$. The two cavities share the same value of the product of pressure and volume.

Amoruso e Crescentini, 2009

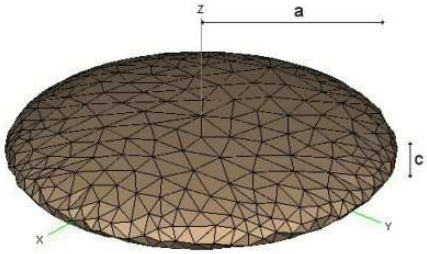

Sill
Aspect-ratio
150-500

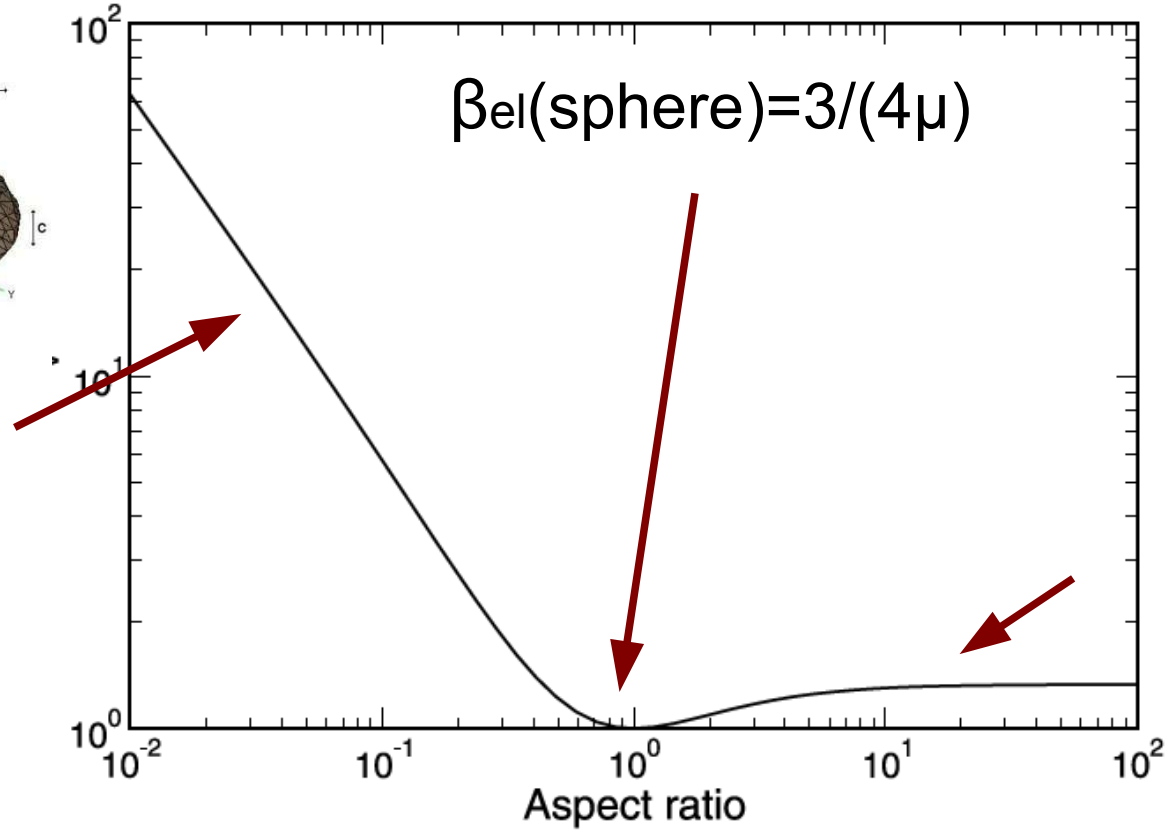

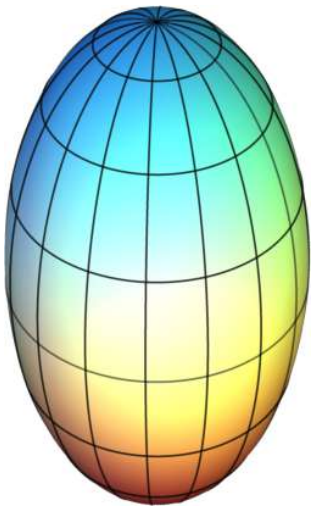

$\beta_{el}^{sheet}=2(1-\nu)a/(\pi\mu c)$

β_{el}(prolate ell)=1/(μ)

Amoruso e Crescentini, 2009

$$dM/dp_{el} = (V d\rho_m + \rho_m dV)/dp_{el} = M\beta$$

$$-dM/dt = k(p - p_a)$$

$$dp/dt = (p + \Delta p_{er} - p_a)/\tau \qquad \tau = (\rho_m V \beta)/k$$

Rivalta et al., submitted

$$V_{out}=k\tau\,(\Delta\rho g d+\Delta p_{el})(1-\exp(-t/\tau))/\rho_m$$

$$V_{out}=V\beta(\Delta\rho g d+\Delta p_{el})=V\beta\Delta p_{er},$$

Rivalta et al., submitted

$$V_{out}/V = (\beta_m + \beta_{el})\Delta p$$

Rivalta et al., submitted

Thermal aspect

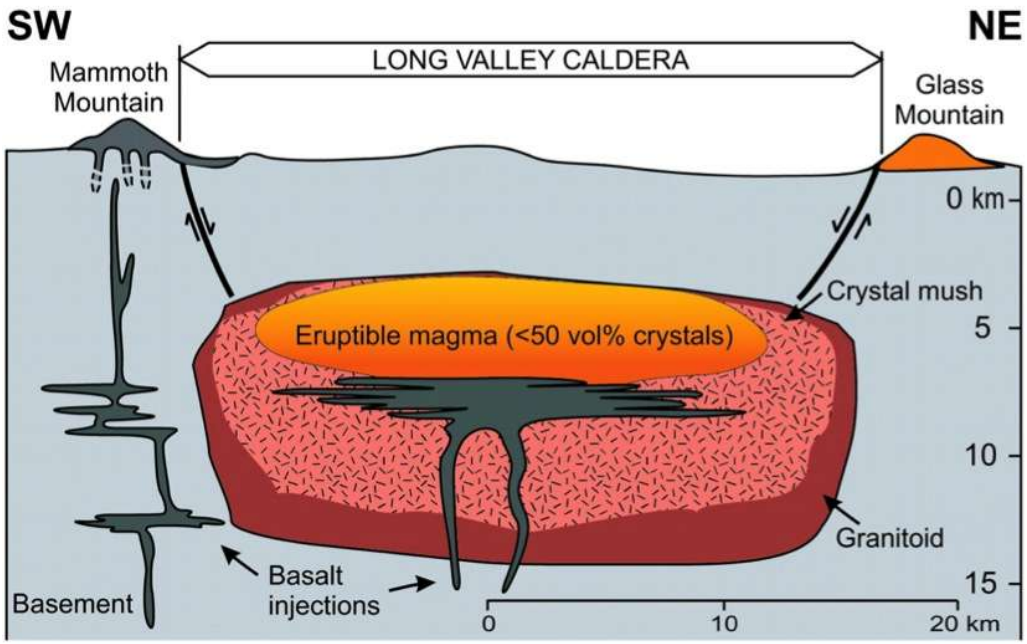

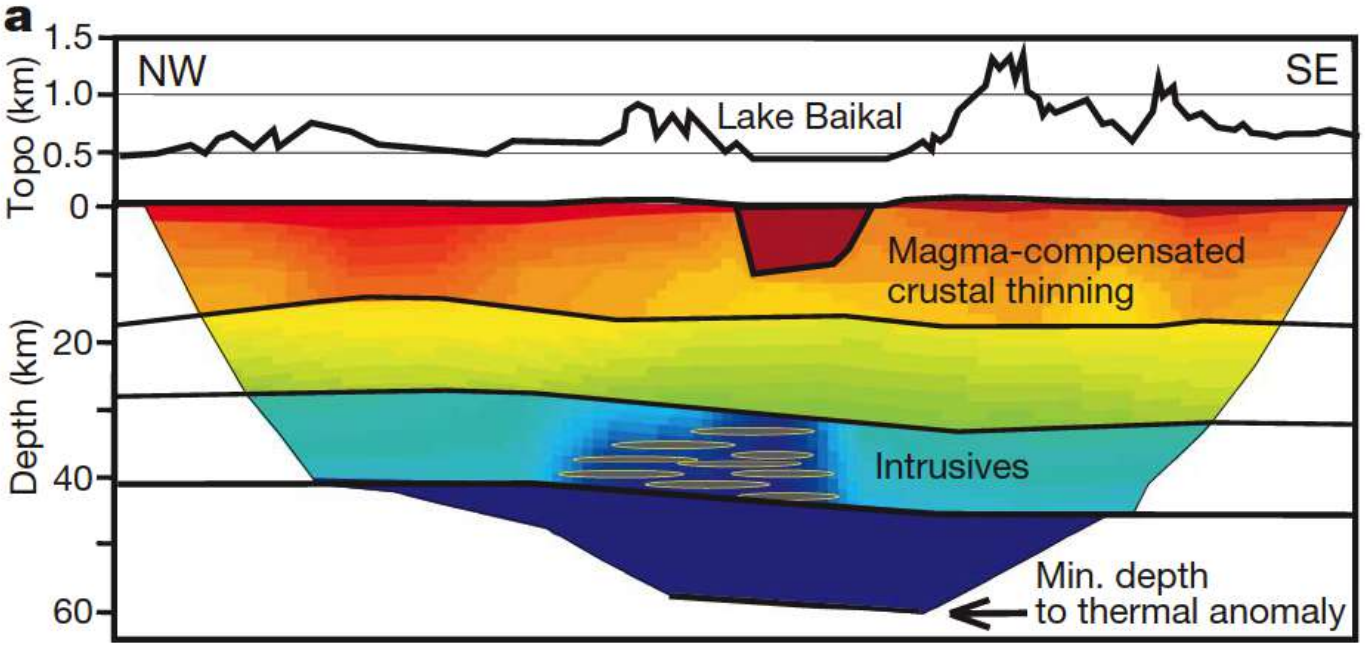

Conclusions and perspectives

- The elevation/loading history of volcanoes or volcanic zones matters: trajectories, storage architecture, depth

- Mechanical models of dike propagation show that surface loads induce deep vertically-developed storage below stratovolcanoes, and shallow horizontally-developed storage below calderas.

- Implications for eruptive potential: larger compressibility (structural and magma compressibility) means large typical eruptive size.